

## **Cocaine-induced neuron subtype mitochondrial dynamics through Egr3 transcriptional regulation**

Shannon Cole<sup>1\*</sup>, Ramesh Chandra<sup>1\*</sup>, Maya Harris<sup>1</sup>, Ishan Patel<sup>1</sup>, Torrance Wang<sup>1</sup>, Hyunjae Kim<sup>1</sup>, Leah Jensen<sup>1</sup>, Scott J Russo<sup>2</sup>, Gustavo Turecki<sup>3</sup>, Amy M Gancarz-Kausch<sup>4, 5</sup>, David M Dietz<sup>4</sup> and Mary Kay Lobo<sup>1#</sup>

<sup>1</sup>Department of Anatomy and Neurobiology, University of Maryland School of Medicine, Baltimore, MD, USA.

<sup>2</sup>Fishberg Department of Neuroscience and Friedman Brain Institute, Graduate School of Biomedical Sciences at the Icahn School of Medicine at Mount Sinai, New York, NY, USA.

<sup>3</sup>McGill Group for Suicide Studies, Douglas Mental Health University Institute, McGill University, Montréal, QC, Canada.

<sup>4</sup>Department of Pharmacology and Toxicology, The Research Institution on Addictions, State University of New York at Buffalo, Buffalo, NY, USA.

<sup>5</sup>Department of Psychology, California State University Bakersfield, Bakersfield, CA, USA

\* Denote co-first author and equal contribution

**#To whom correspondence should be addressed:**

Mary Kay Lobo, PhD

Department of Anatomy and Neurobiology

University of Maryland School of Medicine

20 Penn Street, HSF II Rm S265

Baltimore, MD, 21201, USA

Phone: 410-706-8824

[mklobo@som.umaryland.edu](mailto:mklobo@som.umaryland.edu)

## **Abstract**

Mitochondrial function is required for brain energy homeostasis and neuroadaptation. Recent studies demonstrated that cocaine affects mitochondrial dynamics within the nucleus accumbens (NAc) and mitochondria are differentially regulated by cocaine in dopamine receptor-1 (D1) containing medium spiny neurons (MSNs) vs dopamine receptor-2 (D2)-MSNs. Here, it is demonstrated that cocaine enhances binding of the transcription factor, early growth response factor 3 (Egr3), to nuclear genes involved in mitochondrial function and dynamics. Further, cocaine exposure regulates mRNA of these mitochondria-associated nuclear genes in both contingent or noncontingent cocaine administration and in both rodent models and human postmortem tissue. Interestingly, several mitochondrial genes showed distinct profiles of expression in D1-MSNs vs D2-MSNs, with cocaine exposure generally increasing mitochondrial-associated nuclear gene expression in D1-MSNs vs suppression in D2-MSNs. Subsequent experiments demonstrated that Egr3 overexpression in D1-MSNs enhances the expression of several mitochondrial-associated nuclear genes. By contrast, blunting Egr3 expression blocks cocaine enhancement of the mitochondrial-associated transcriptional coactivator, peroxisome proliferator-activated receptor gamma coactivator (PGC1 $\alpha$ ), and the mitochondrial fission molecule, dynamin related protein 1 (Drp1). Finally, reducing Egr3 expression attenuates the cocaine-induced enhancement of small-sized mitochondria, demonstrating that Egr3 regulates mitochondrial morphological adaptations. Collectively, these studies demonstrate cocaine exposure impacts Egr3 transcriptional regulation of mitochondria-related nuclear gene transcripts and mitochondrial dynamics, with implications for mechanisms underlying neuronal function and plasticity occurring with cocaine exposure.

**Key words:** cocaine, D1-MSNs, D2-MSNs, mitochondria, nucleus accumbens

## **Introduction**

Mitochondria are the chief energy producing unit of the cell through cellular respiration; a requirement for basic mammalian life function and cellular adaptation. Only recently have studies revealed the important relationship of mitochondrial programming, machinery, and adaptations in brain responses to drugs of abuse in humans and in rodent models<sup>1-3</sup>. In the nucleus accumbens (NAc) mitochondrial fission or molecules related to mitochondrial dynamics and function are altered by cocaine<sup>1,2</sup>. The NAc is a critical hub involved in motivation for various rewards, such as food, sex, and drugs of abuse, as well as fear and aversion<sup>4,5</sup>.

The NAc is primarily comprised of medium spiny neurons (MSNs; a.k.a. spiny projection neurons) of two distinct subpopulations: D1-dopamine receptor expressing MSNs (D1-MSNs) and D2-dopamine receptor expressing MSNs (D2-MSNs)<sup>6,7</sup>. D1- and D2-MSN activity and morphology are altered across multiple pathological states, such as addiction, stress, depression, and pain<sup>8-12</sup>.

Studies into NAc molecular neurobiological mechanisms have revealed that gene transcripts and protein expression involved in neuroplasticity often differ between D1- and D2-MSNs in response to cocaine<sup>12-20</sup>. Further, patterns of gene regulation specific to mitochondrial-related genes can be distinct and opposing between these neuron populations<sup>1,2</sup>. For instance, following cocaine exposure or self-administration the mitochondrial fission protein, dynamin related protein (Drp1), and a transcriptional coactivator molecule involved with mitochondrial dynamics, peroxisome proliferator-activated receptor gamma coactivator (PGC1 $\alpha$ ), are enhanced in D1-MSNs and decreased in D2-MSNs<sup>1,2,21,22</sup>. Interestingly, recent studies have discovered that mitochondrial fission via Drp1 is required for neuronal spine

formation<sup>23,24</sup>; a key morphological adaptation for enhancing synaptic strength and thought to underpin the craving and seeking of drugs long after consumption has ceased<sup>25-33</sup>.

Another NAc neurobiological dichotomy has been observed in drug-responsive genes upstream of mitochondrial factors. One such transcription factor is early growth response factor 3 (Egr3), which regulates several cocaine-associated genes, such as CREB, CamKII $\alpha$ , and  $\Delta$ FosB<sup>14</sup>. Egr3 displays opposing function in D1-MSNs vs D2-MSNs: it is upregulated in D1-MSNs in response to repeated cocaine and is necessary for cocaine conditioned place preference (CPP) and cocaine induced psychomotor locomotion. In contrast, D2-MSNs have a reduction in Egr3 in response to repeated cocaine and enhancement of Egr3 in these neurons decreases cocaine CPP and psychomotor locomotion. The effect of Egr3 in D2-MSNs is also observed after long term abstinence, but in a sex-specific manner. In females, enhanced D2-MSN Egr3 precipitated cocaine extinction and blocked cocaine-induced reinstatement, whereas males perseverated nose poking during extinction and showed heightened response to reinstatement<sup>34</sup>. The effects of Egr3 on cocaine-regulated behaviors could occur through mitochondrial processes, since cocaine exposure enhances Egr3 binding to the PGC1 $\alpha$  promoter in NAc<sup>2</sup>. Collectively, these findings suggest an important link between Egr3 transcription, molecules involved with mitochondrial processes, and the facilitation of cocaine-induced behaviors.

What remains largely unexplored is the relationship between drug-exposure and transcription factors impacting mitochondrial processes. This study assayed the impact of cocaine exposure on Egr3 and multiple downstream target nuclear genes that regulate mitochondrial related transcription, dynamics, and function in the NAc of mice. Additionally, a number of these mitochondrial-related nuclear genes were assayed following contingent or non-contingent cocaine exposure in rodents and were also examined in postmortem NAc of cocaine

dependents. Further, the link between Egr3 and mitochondrial-related nuclear genes was further parsed in NAc D1-MSNs vs D2-MSNs. Mitochondrial-related nuclear gene classes included: the general transcription factors nuclear respiratory factor 1 and 2 (nrf1 and nrf2); a transcriptional coactivator of mitochondrial related nuclear genes, PGC1 $\alpha$ ; mitochondria-specific transcription factors A and b1 (tfam and tfb1); the mitochondrial trafficking membrane protein, translocase of the outer mitochondrial membrane 20 (tom20); the mitochondrial fission regulator, Drp1; and a mitochondrial DNA polymerase subunit gamma, Pol $\gamma$ . Together, these studies examine the impact of cocaine exposure on Egr3 transcriptional regulation of mitochondria-related nuclear gene transcripts and mitochondrial dynamics.

## **Materials and Methods**

### **Animals and Human Postmortem Samples**

All animals experiments and handling followed guidelines set by the Institutional Animal Care and Use Committee (IACUC) at The University of Maryland School of Medicine and The University at Buffalo, The State University of New York. In both institutions, the health status of test animals was closely monitored by onsite veterinary staff and the experimenters throughout all experiments. All mice were maintained on a 12h light/dark cycle ad libitum food and water. Mice were group housed (3-5 per cage) for all experiments. D1-Cre hemizygote or D2-Cre hemizygote bacterial artificial chromosome (BAC) transgenic male mice from GENSAT (Line KG139)<sup>35</sup> ([www.gensat.org](http://www.gensat.org)) on a C57BL/6J background were used for Egr3 enhancement and quantitative RT-PCR analysis; D1-Cre mice were used for qRT-PCR analysis for Egr3-miR experiments and mitochondrial morphology analysis. Homozygous RiboTag (RT) mice on a C57BL/6J background, expressing a Cre-inducible HA-Rpl22 (Sanz et al., 2009) were crossed to

D1-Cre or D2-Cre mouse lines to generate D1-Cre-RT and D2-Cre-RT male mice<sup>1</sup> and used for cell type-specific ribosome-associated mRNA isolation. Data for saline control mice used in RT experiments came from<sup>36</sup>. RiboTag testing comprised of samples from D1-Cre-RT and D2-Cre-RT mice, ages 8-10 weeks with 4 mice pooled per sample. Animal numbers were determined based on previous studies<sup>1,2,14</sup>. Four to five D1-Cre mice per group, age 10-12 weeks, were used for mitochondrial morphological analysis. Naive male Sprague-Dawley rats (250-275 g at the beginning of the experiment), used for self-administration cDNA, were maintained on a 12h reverse light/dark cycle ad libitum food and water. After catheterization surgery, rats were single housed for the duration of the experiments. For all *in vivo* studies, animals were randomly assigned to the treatment or control group.

Human postmortem tissue was also used in<sup>1</sup> and was handled according to the same storage and treatment protocols. The cohort of cocaine-dependent individuals comprised of 24 males and 2 female between ages 20 and 53 years (see Table S1 from<sup>1</sup> for individual subject details). All subjects died suddenly without a prolonged agonal state or protracted medical illness. The causes of death were ascertained by the Quebec Coroner Office. A toxicological screen was conducted with tissue samples to obtain information on medication and illicit substance use at the time of death. The cocaine-dependent subject group consisted of 14 individuals who met the Structured Clinical Interview for Diagnostic and Statistical Manual of Mental Disorders-IV (DSM-IV) Axis I Disorders: Clinician Version (SCID-I) criteria for cocaine dependence. The control group comprised 12 subjects with no history of cocaine dependence and no major psychiatric diagnoses. The processing of the tissue is outlined in previous publications<sup>37,38</sup>. Hemispheres were immediately separated by a sagittal cut into 1cm-thick slices and placed in a mixture of dry ice and isopentane (1:1; vol:vol). The frozen tissue was then stored at 80C.

## **Mouse stereotaxic surgery**

Mice were anesthetized using 4% isoflurane in a small induction chamber. After initial induction, isoflurane was maintained at 1-2% for the remainder of the surgery. Animals were placed in a stereotaxic instrument and their skull was exposed. 33 gauge Hamilton syringe needles were used to inject Cre-inducible double inverted open (DIO) reading frame adeno-associated viruses (AAV) <sup>1</sup> into the NAc of test animals. AAV-DIO-Egr3-EYFP was used to over express Egr3 or a control AAV-DIO-EYFP in D1 and D2-Cre mice. To label mitochondria AAV-DIO-mito-dsRed was injected in tandem with either AAV-DIO-Egr3-miR-IRES-mCitrine for Egr3 knockdown or AAV-DIO-Scramble(SS)-miR-IRES-mCitrine viral control <sup>1,2,14,36</sup> in D1-Cre-RT mice.

All experiments involving viral infusion had virus injected bilaterally into the NAc (anterior/posterior, AP+1.6; medial/lateral, ML  $\pm$  1.5; dorsal/ventral, DV-4.4, 10 degree angle). Mice were then returned to the vivarium for 2 weeks to allow for recovery and virus expression. All viruses were packaged in lab facilities as previously described <sup>1</sup>.

## **RiboTag and qRT-PCR procedure**

NAc samples were pooled from four (4) D1-Cre-RT and D2-Cre-RT male and female mice and RNA isolation from immunoprecipitated polyribosomes using primary mouse anti-HA antibody (Covance Research Products, Cat#MMS101R) and secondary antibody coated magnetic Dynabeads (Dynabeads protein G, Invitrogen) to pulldown the MSN specific RNA. Immunoprecipitated polyribosomes and non-immunoprecipitated input was prepared according to our previous studies <sup>1,14,36</sup> RNA from polyribosome immunoprecipitated samples or input was subsequently extracted using the Total RNA Kit (Omega) according to manufacturer's

instructions. For cDNA synthesis, qRT-PCR, and analysis we follow the steps as described previously (Chandra, Engeln et al., 2017; Chandra et al., 2015). The list of primers used in this study are mDrp1-Forward GGGCACTTAAATTGGGCTCC, mDrp1-Reverse TGTATTCTGTTGGCGTGGAAC, mNrf2- Forward TCTACTGAAAAGGCGGCTCA, mNrf2- Reverse TTGCCATCTCTGGTTTGCTG, mNRF1- Forward AGACCTCTGCTAGATTCACCG, mNRF1-Reverse CCTGGACTTCACAAGCACTC, mPolG-Forward ACTCCTGGAACAGTTGTGCT, mPolG- Reverse CGTCCATCTACTCAGGACGG, mTFAMSV1- Forward GCAGGCACTACAGCGATAACA, mTFAMSV1- Reverse GCCTCTACCTTTCCCATTC, mTFB1- Forward TACGCCCTTGATAGAGCCCA, mTFB-Reverse TCCTTCGAAACTGAAACGCA, mTom20- Forward CTGTGCTCTGGGCACTTAAC, mTom20-Reverse AGGGTGCACACAGGTCTAAT, mGapdh-Forward AGGTCGGTGTGAACGGATTTG, mGapdh-Reverse TGTAGACCATGTAGTTGAGGTCA. rDrp1-Forward CTCCACCTTTTGAAGCCAGG, rDrp1-Reverse GCAGCCGTAGTCCTCAAAGA, rNrf2- Forward CCGTACAAAACAAACTAGCTC, rNrf2- Reverse AGATGGCAACGTGTTTCCTTG, rNRF1- Forward ATGGCGGAAGTAATGAAAGACG, rNRF1-Reverse TACTTCCCAGCAGCCTTAGC, rPolG- Forward CTCCGCACCCGAAGATTTG, rPolG- Reverse CCTCCTCAGAGAATGGGCAG, rTFAMSV1- Forward ATCAAGACTGTGCGTGCATC, rTFAMSV1- Reverse AGAACTTCACAAACCCGCAC, rTFB1- Forward TGAAGACCCACAACCTTTTGC, rTFB1-Reverse CAGCAGTTAGAACCCACAGC, rTom20- Forward TGGAATGAGCCAGACACCAA, rTom20-Reverse CACAGTTTGCCCTTATCCCC, rGapdh-Forward TGGCCTCCAAGGAGTAAGAA, rGapdh-Reverse TGTGAGGGAGATGCTCAGTG.



hDrp1-Forward TCTTGGAGGACTATGGCAGC, hDrp1-Reverse  
CAAAGCAGTTTGCCTGTGGA, hNRF1- Forward GGTGCGCTGTGGAAACAATA, hNRF1-  
Reverse CAGTAGCTCAACGCATGACC, hPolG- Forward TCACCAAAGGCTCCTTGAA,  
hPolG- Reverse CACGGGAGCAAATACAGAGC, hTFAMSV1- Forward  
GGCACAGGAAACCAGTTAGG, hTFAMSV1- Reverse ATGCTGGCAGAAGTCCATGA,  
hTFB1- Forward TGCACTACGTGGAGCTTCTT, hTFB1-Reverse  
GTCACATCTGGTCATTGGCA, hTom20- Forward TAGCCTTGTGAGCTTCGCTA,  
hTom20-Reverse CAGCAGACGCATTCTCTCAC, hGapdh-Forward, and hGapdh-Reverse.  
Samples were run with experimenters blind to conditions. mRNA expression changes were  
measured using quantitative polymerase chain reaction (qPCR) with PerfeCTa SYBR Green  
FastMix (Quanta). Quantification of mRNA changes was performed using the  $-\Delta\Delta$  CT method,  
using glyceraldehyde 3-phosphate dehydrogenase (GAPDH) as a housekeeping gene, and  
immunoprecipitated samples were then normalized to the averaged input from the respective  
MSN subtype.

### **Chromatin immunoprecipitation (ChIP)**

Fresh NAc punches were prepared for ChIP as previously described with minor  
modifications<sup>2,14</sup> Briefly, four 14-gauge NAc punches per C57BL/6J mouse (four animals  
pooled per sample) were collected, cross-linked with 1% formaldehyde and quenched with 2 M  
glycine before freezing at  $-80^{\circ}\text{C}$ . Before sample sonication, IgG magnetic beads (Invitrogen;  
sheep anti-rabbit, cat.# 11202D) were incubated with an anti-Egr3 (rabbit polyclonal, Santa Cruz  
Biotech, cat.# SC-191, 8–10  $\mu\text{g}$  per reaction) antibody overnight at  $4^{\circ}\text{C}$  under constant rotation  
in blocking solution (0.5% w/v BSA in 1X PBS). The chromatin was fragmented by sonication

to an average length of 500-700bp. After sonication, equal concentrations of chromatin were transferred to new tubes and 100µl of the final product was saved to for input controls. Following the washing and resuspension of the antibody–bead conjugates, antibody–bead mixtures were added to each chromatin sample (600µl) and incubated for ~16 h under constant rotation at 4°C. Samples were then washed and reverse cross-linked at 65°C overnight and DNA was purified using a PCR purification kit (QIAGEN). After DNA purification, samples were used for qPCR analysis and normalized to their appropriate input controls as previously described (Maze I science 2010, Chandra 2015). Rabbit IgG immunoprecipitation control sample was prepared by adding blocking buffer to magnetic beads instead an anti-Egr3 for appropriate enrichment of Egr3 ChIPs, >1.5 fold. The promoter primer sequences are Drp1 forward CCCACCTCTGTCGTGGC, Drp1 reverse TTGCTTCCTCTTCTCCTCCG, Nrf1 forward GCTTTGTACCAAAGTTCCCCG, Nrf1 reverse CCTCGACCCCTCTCTGAAATG, Nrf2 forward AGCCTTTTCTCCGCCTCTAA, Nrf2 reverse CTAGGAGATAGCCTGCTCGC, polg forward GCAGACGGGAAGTTGCG, polg reverse TTCTGCGGCAGCCCAC, tfam forward CGCATCCCCTCGTCTATCAG, tfam reverse GGAGGACGAGGGTGGGA, tfb1 forward AGAAGTAATGGACGCGAAGAAA, tfb1 reverse ATGGTGATTGGTTGCTTGCT, Tom20 forward TGGTGCTGCATTCCCTAAGT, Tom20 reverse GAATCAGCCTTGGCTTCCTG.

### **Immunohistochemistry**

Mice were perfused with 0.1M phosphate buffered saline (PBS) followed by 4% paraformaldehyde (PFA). Brains were immersed in azide PBS overnight. Brains were dissected with a vibratome (Leica) at 100 µm into PBS for mitochondria counting or sectioned on a vibratome (Leica). After washing with PBS, regular immunostaining protocol was followed. Brain sections were blocked in 3% normal donkey serum with 0.3% Triton-X for 30 min at room

temperature. Sections were then incubated overnight in a cold in primary antibody 1:1500 chicken anti-GFP (Aves Labs, Cat#GFP-1020) diluted in the 3% NDS and 0.3% tween 20 solution. On the second day, tissue sections were rinsed in PBS three times for 30 min per rinse followed by another 8-hour wash by rinsing with PBS every hour at room temperature. Overnight incubation in a cold in secondary antibodies, 1:500 donkey anti-chicken-Alexa488 (Jackson ImmunoResearch cat# 703-545-155). DsRed was not amplified via immunostaining, as endogenous virus expression was sufficient for imaging sections were rinsed in PBS every hour for 8 hours. Finally, slices were mounted on slides and left to dry overnight in the dark and cover slipped next day with mounting media.

### **Mitochondrial Imaging and Analysis**

Detailed methods for mitochondrial imaging are described in <sup>1</sup> Sections were imaged on a Olympus Bx61 confocal microscope. A total of 4-5 cells were imaged per mouse by confocal scanning. High-resolution Z-stacks images were obtained with 0.4mm increments using a 60x oil immersion objective with 2x digital zoom. Sections were scanned for neuron distal dendrites (over 100 mm radius from the soma) and distal secondary dendrites (the first nearest branch from distal dendrite). Using a three-dimensional (3D) image reconstruction which permits easy examination of cell structures and dendritic mitochondria morphology we analyzed multiple mitochondrial morphological parameters using Imaris 8.3 software (Bitplane). Mitochondrial analysis was performed blinded to the condition.

### **Statistical analysis**

Graphpad Prism 6.0 software was used for statistical analysis. Two-way ANOVA was used for mitochondrial size frequency analysis followed by Bonferroni post-hoc correction. Student's t-test was used for all other experiments. Comparisons were tested for normalcy.

Significance was established when p-values were below 0.05. All graphs represent mean  $\pm$  standard error (SEM). For qRT-PCR data, Grubbs outlier test was performed on data with obvious outliers and no more than one animal or sample was removed per group.

## **Results**

Egr3 binding sites are found on promoters of many mitochondrial-related gene (gene-regulation.com, Alibaba), thus we performed ChIP to determine whether cocaine exposure alters Egr3 binding to the promoters of these mitochondrial-related nuclear genes (Fig 1a). Following 7-days of i.p. cocaine injection (20mg/kg) NAc tissue was collected 24 hours after the last injection (Fig 1b), a time point shown to induce transcriptional and cellular plasticity in NAc<sup>2,14,20,39-41</sup>. In bulk NAc tissue, enhanced binding of Egr3 was observed on the promoters of the mitochondrial fission molecule, Drp1, the transcription factor, nuclear respiratory factor nrf2, and the DNA polymerase gamma subunit (poly $\gamma$ ). This data is in line with our previous study that demonstrated enhanced Egr3 binding at the PGC1 $\alpha$  promoter in NAc after repeated cocaine<sup>2</sup>. Trending elevations in Egr3 enrichment on promoters for mitochondrial transcription factors, tfam and tfb1, and the mitochondrial trafficking membrane protein, Tomm20 were also seen (Fig1b). These findings implicate cocaine-mediated Egr3 transcriptional regulation of mitochondrial-related nuclear genes.

Next, qRT-PCR was used to quantify mitochondria-related transcripts in bulk NAc tissue to determine if a history of cocaine exposure alters the expression of the mitochondria-related genes examined above. Mice receiving 7-days of i.p. cocaine (20mg/kg) injections showed an increase in nrf1, nrf2, and tomm20, with trending enhancement in tfam and tfb1 (see Fig 2a & Table 1). Rats that self-administered cocaine for 10-days (1mg/kg/infusion) showed similar patterns, with enhancements in nrf1, tfb1, and tomm20, and trending enhancements in nrf2, poly $\gamma$ ,

and tfam (see Fig 2b & Table 1). To compare rodent models with cocaine-dependent individuals, postmortem human tissue was analyzed for the same mitochondria-related nuclear genes. Tissue from cocaine-dependents had enhanced nrf2 and displayed trending enhancement in nrf1 and Tomm20 (see Fig 2c & Table 1). The increase in nrf1 is consistent with our previous studies demonstrating increased Drp1 and PGC1 $\alpha$  in NAc of the same cocaine dependent cohort.

Egr3, Drp1, and PGC1 $\alpha$  have been shown to be oppositely enhanced in D1-MSNs vs D2-MSNs following repeated cocaine exposure<sup>14</sup>, and mitochondrial morphology at baseline and after repeated cocaine is different between D1 and D2-MSNs<sup>1,2,36</sup>. Thus, next examined were mitochondrial-related nuclear genes in D1 vs D2-MSNs. An established RiboTag approach was used to examine mRNA from NAc of D1-Cre-RiboTag (RT) or D2-Cre- RiboTag (RT) mice (Fig 3a). D1-Cre-RT mice receiving 7-days of i.p. cocaine injections (20mg/kg) showed an increase in TFAM and strongly trending expression of TFB1 and Tomm20 mRNA in NAc D1-MSNs (Fig 3b). By contrast, D2-Cre-RT mice showed a reduction in mRNA levels of Poly, TFAM, TFB1, and Tomm20 in NAc D2-MSNs after repeated cocaine (Fig 3c). These data are consistent with our previous study demonstrating that Drp1 and PGC1 $\alpha$  are enhanced in NAc D1-MSNs and reduced in D2-MSN after repeated cocaine exposure<sup>2</sup>.

Next, examined was the effect of Egr3 overexpression on mitochondrial-related nuclear gene expression in NAc by infusing a AAV-DIO-Egr3-EYFP virus or AAV-DIO-EYFP into the NAc of D1-Cre or D2 Cre- mice that received had prior cocaine exposure including repeated cocaine injections (10mg/kg). A lower dose of 10mg/kg cocaine was used compared to 20mg/kg to determine if Egr3 overexpression in each MSN subtype potentiated the effects of cocaine. Enhancing Egr3 in D1-MSNs of mice that received repeated cocaine injections resulted in an increase of Drp1, PGC1 $\alpha$ , Tfam, and Tomm20, with trending enhancements for nrf1 and poly in

NAc compared to mice that also received repeated cocaine but EYFP control virus (Fig 4a).

These findings are consistent with the ChIP results showing an increase in Egr3 enrichment on mitochondria-related nuclear gene promoters. Further, we detected no change in mitochondrial-related nuclear genes when Egr3 was overexpressed in D2-MSNs under repeated cocaine conditions (Fig 4b).

Considering that enhancement of Drp1 and PGC1 $\alpha$  in NAc D1-MSNs and enrichment of Egr3 on these promoters in NAc occurs under repeated exposure cocaine conditions we next determined if reducing Egr3 in D1-MSNs would alter repeated cocaine-induced expression of these mRNA in these neurons. D1-Cre-RT mice received NAc injections of AAV-DIO-Egr3-miR or AAV-DIO-SS-miR followed by repeated cocaine (20mg/kg for 7 days) or saline followed by a 24-hour abstinent period (Fig 5a). D1-Cre-RT mice that received Egr3-miR injections into NAc showed 5-fold lower PGC1 $\alpha$  mRNA (Fig 5b) and 6-fold lower Drp1 mRNA (Fig 5c) in D1-MSNs following cocaine injections compared to SS-miR controls that also received cocaine. Egr3-miR cocaine mice also showed no difference compared to Egr3-miR saline controls in either PGC1 $\alpha$  or Drp1 mRNA. These findings corroborate the model of Egr3 transcriptional regulates mitochondrial-related nuclear genes and is consistent with increased Egr3 binding on promoters of Drp1 (Fig 1) and PGC1 $\alpha$  following cocaine exposure<sup>2</sup>.

Previously, it was demonstrated that Drp1 mediates enhanced mitochondrial fission in D1-MSN dendrites following repeated cocaine exposure, including self-administration and that blockade of Drp1 prevents fission in these neurons<sup>1</sup>. Since our data implicates Egr3 transcriptional regulation of Drp1 in D1-MSNs under repeated cocaine conditions we next examined the impact of Egr3 reduction on cocaine-induced mitochondrial fission. D1-Cre mice received NAc AAV-DIO-Egr3-miR or AAV-DIO-SS-miR along with expressing AAV-DIO-

mito-dsRed<sup>1,36</sup> to label mitochondria in D1-MSNs subtypes, and to allow quantification of mitochondrial volume, density, and size (Fig 6a-b). Following 7-days of i.p. cocaine injections (20mg/kg) or saline brain tissue was collected 24-hours after the last injection. An increase in the frequency of smaller length mitochondria was observed in cocaine treated mice in dendrites, relative to saline treated mice, consistent with our previous finding (Fig 6c; Ramesh Chandra, Engeln, Schiefer, et al., 2017). However, the frequency of small-sized mitochondria was decreased by approximately 30% in Egr3-miR cocaine exposed mice relative to both Egr3-miR and SS-miR saline viral controls. SS-miR controls treated with cocaine showed the highest frequency in the 1.5-3.0 $\mu$ m length bracket, whereas Egr3-miR mice treated with cocaine showed about half as many of these small-sized mitochondria (Fig 6c Two-way ANOVA: Interaction- $F_{(15,70)}=5.07$ ,  $p=0.0001$ , Bonferroni post hoc:  $*p<0.05$ ,  $**p<0.01$ ,  $***p<0.001$ ). By contrast, Egr3-miR mice treated with cocaine showed the most large-sized mitochondria in the 4.5-6 size bracket. A two-way ANOVA revealed differences in mitochondrial volume by drug and virus condition with Egr3-miR mice showing lower volume than SS-miR mice. (Fig 6f; Two-way ANOVA  $F_{(1,14)}=0.4792$ ;  $p=0.5001$ ;  $n=4-5$  per group. Error bars, SEM). Thus, Egr3 expression seems to be necessary for cocaine-induced small-sized mitochondria. Taken together, cocaine-induced gene regulation and mitochondrial structural characteristics are substantially altered in NAc D1-MSNs. These findings align with previous work showing that manipulation of Drp1 dictates mitochondrial morphology characteristics following cocaine self-administration<sup>1</sup>.

## **Discussion**

This study identified distinct gene expression profiles of mitochondrial-related nuclear genes and that Egr3 serves as an upstream transcriptional regulator of these processes in NAc

after cocaine exposure. Overall, the observed gene transcription responses to cocaine across species, route of drug administration, and neuron subpopulation emphasizes the importance of examining neurobiological mechanisms with multiple levels of focus.

Mitochondrial-related nuclear genes with Egr3 promoter binding sites include the mitochondrial fission regulator Drp1; mitochondrial-related transcription factors nrf1 and nrf2; the mitochondrial-related transcriptional coactivator Pgc1 $\alpha$ ; mitochondrial transcription factors tfam and tfb1; DNA polymerase subunit gamma (pol $\gamma$ ); and outer membrane transport protein, tomm20<sup>22,42-46</sup>. Repeated cocaine exposure resulted in upregulated Egr3 binding to mitochondria-related nuclear gene promoters in NAc. This is in alignment with our previous study showing Egr3 binding on PGC1 $\alpha$  is enhanced following cocaine exposure<sup>2</sup>. Subsequent tests examined mRNA of Egr3-target mitochondrial nuclear genes in NAc. Here, both mice receiving cocaine injections and rats self-administering cocaine showed similar patterns of gene expression, with enhanced nrf1, nrf2, and tomm20, but only nrf2 was upregulated in postmortem tissue of cocaine dependents, in contrast with mRNA levels in rodent models. Additionally, other studies have shown that cocaine upregulates the mitochondrial fission genes, Drp1 and PGC1 $\alpha$ <sup>1,2</sup>, in bulk NAc tissue; including cocaine enhancement of Drp1 mRNA in both rodent models and humans<sup>1</sup>.

What might account for the disparity here between rodents and humans? Factors, such as route of cocaine administration, methods of extraction, and potential co-morbid mental disorders in human subjects, such as major depression or bipolar disorder (See Table S1 in<sup>1</sup>). These differences may reflect neuropsychopathological differences in genotype and phenotype regulation patterns in the NAc and in MSN subtypes linked to broad forms of neuropathology<sup>9-</sup>



<sup>11,47-49</sup>. Additionally, the analysis in bulk tissue could mask cell subtype specific effects that we have observed in rodent tissue.

Analysis of NAc MSN subtypes demonstrated upregulation of mitochondria-related mRNAs in D1-MSNs, whereas D2-MSNs displayed a general decrease in mitochondria-related mRNAs. In comparison to bulk NAc tissue quantification, these findings demonstrate the importance of localizing and characterizing gene regulation to specific neuron subtypes within regions of interest. Further, our findings are consistent with a previous study demonstrating increases in Drp1 expression and increased frequency of small mitochondria in D1-MSNs, while lower levels of Drp and increased larger mitochondrial frequency are observed in D2-MSNs following cocaine exposure or self-administration <sup>1</sup>. Moreover, PGC1 $\alpha$  also shows enhancement in D1-MSNs and a decrease in D2-MSNs following 7 days of cocaine administration <sup>2</sup>. Thus, these findings further elucidate the differences of additional mitochondrial-related molecules in MSN subtypes following repeated cocaine exposure.

The finding that Egr3 enhancement increases multiple mitochondrial-related genes in D1-MSNs, but not D2-MSNs, is in line with the above findings and previous work showing D1-specific enhancement of Egr3, PGC1 $\alpha$ , and Drp1 <sup>1,2</sup>. The difference in regulation between these neuron populations highlights an important principle: D1-MSNs vs D2-MSNs may differentially regulate mitochondrial genes in response to cocaine and enhancement of Egr3 in D1-MSNs appears to potentiate the effects of cocaine exposure on mitochondrial nuclear gene expression. The subsequent disruption of Egr3 by NAc infusion of Egr3-miR into D1-Cre mice prevented cocaine-mediated enhancement of Drp1 and PGC1 $\alpha$ . These findings corroborate the model of Egr3 transcriptional regulation of mitochondrial nuclear genes and previous findings showing cocaine enhancement of Egr3-PGC1 $\alpha$  binding <sup>2</sup>.

Egr3 blockade in D1-MSNs prevented cocaine-induced fission, as indicated by reduced frequency of small-sized mitochondria. As cocaine exposure resulted in increased Egr3 binding to the Drp1 promoter and Egr3 blockade prevented cocaine-induced upregulation of Drp1 in D1-MSNs, it appears that Egr3 transcriptional regulation of Drp1 is necessary for the D1-MSN Drp1-mediate mitochondrial fission occurring with cocaine exposure. Drp1 has also been shown to be necessary for the formation of dendritic spines<sup>23,24</sup>. Thus, converging lines of evidence support the hypothesis that cocaine-induced neuroplasticity in NAc could be directly tuned by Egr3 regulation of mitochondrial dynamics. Given a large literature demonstrating enhanced excitatory plasticity and signaling processes in D1-MSNs with both contingent and non-contingent chronic cocaine it is plausible that these neurons require higher energy demands<sup>13,17-20,50</sup> or mitochondria could be acting as buffers of calcium homeostasis required for neuroplasticity events<sup>23</sup>.

## **Conclusion**

In sum, this study 1) identifies the direct link between cocaine-associated transcription factors, such as Egr3, and mitochondrial dynamics, and 2) further profiles the regulation of several mitochondria-related nuclear genes following cocaine exposure. Our studies further demonstrate that patterns of mitochondria-related nuclear gene expression following cocaine exposure depends upon specific cell populations, with enhancement of many mitochondrial-related nuclear genes in D1-MSNs and reduction in D2-MSNs. Moreover, Egr3 is a key mechanism in D1-MSNs that is required for cocaine to enhance mitochondrial-associated nuclear gene expression. Finally, the blockade of Egr3 prevents cocaine-induced alterations in D1-MSN mitochondrial fission. Taken together, these findings establish that Egr3 directly regulates

enhancement of mitochondrial dynamics, which may underlie behaviors occurring in rodent models and human substance use disorder. Our studies provide a model for how cocaine-associated transcription factors control mechanisms of mitochondrial dynamics that potentially underlie neurobiological adaptations to drugs of abuse.

### **Acknowledgements**

The authors would like to thank N.G. Larsson (Max Planck Institute for Biology of Ageing, D-50931 Cologne, Germany) for supplying the mito-dsRed vector used in this study. This work was supported by NIH R01DA038613.

### **References**

1. Chandra R, Engeln M, Schiefer C, et al. Drp1 Mitochondrial Fission in D1 Neurons Mediates Behavioral and Cellular Plasticity during Early Cocaine Abstinence. *Neuron*. 2017;96(6):1327-1341.e6. doi:10.1016/j.neuron.2017.11.037
2. Chandra R, Engeln M, Francis TC, Konkalmatt P, Patel D, Lobo MK. A Role for Peroxisome Proliferator-Activated Receptor Gamma Coactivator-1alpha in Nucleus Accumbens Neuron Subtypes in Cocaine Action. *Biol Psychiatry*. 2017;81(7):564-572. doi:10.1016/j.biopsych.2016.10.024
3. Cunha-Oliveira T, Silva L, Silva AM, Moreno AJ, Oliveira CR, Santos MS. Mitochondrial complex I dysfunction induced by cocaine and cocaine plus morphine in brain and liver mitochondria. *Toxicol Lett*. 2013;219(3):298-306. doi:10.1016/j.toxlet.2013.03.025
4. Volkow ND, Koob GF, McLellan AT. Neurobiologic Advances from the Brain Disease

- Model of Addiction. *N Engl J Med*. 2016;374(4):363-371. doi:10.1056/NEJMra1511480
5. Baumgartner HM, Cole SL, Olney JJ, Berridge KC. Desire or Dread from Nucleus Accumbens Inhibitions: Reversed by Same-Site Optogenetic Excitations. *J Neurosci*. 2020. doi:10.1523/JNEUROSCI.2902-19.2020
  6. Gerfen CR, Engber TM, Mahan LC, et al. D1 and D2 dopamine receptor-regulated gene expression of striatonigral and striatopallidal neurons. *Science* (80- ). 1990;250(4986):1429-1432.
  7. Smith RJ, Lobo MK, Spencer S, Kalivas PW. Cocaine-induced adaptations in D1 and D2 accumbens projection neurons (a dichotomy not necessarily synonymous with direct and indirect pathways). *Curr Opin Neurobiol*. 2013;23(4):546-552. doi:10.1016/j.conb.2013.01.026
  8. Fox ME, Chandra R, Menken MS, et al. Dendritic remodeling of D1 neurons by RhoA/Rho-kinase mediates depression-like behavior. *Mol Psychiatry*. August 2018. doi:10.1038/s41380-018-0211-5
  9. Francis TC, Chandra R, Friend DM, et al. Nucleus accumbens medium spiny neuron subtypes mediate depression-related outcomes to social defeat stress. *Biol Psychiatry*. 2015. doi:10.1016/j.biopsych.2014.07.021
  10. Massaly N, Copits BA, Wilson-Poe AR, et al. Pain-Induced Negative Affect Is Mediated via Recruitment of The Nucleus Accumbens Kappa Opioid System. *Neuron*. 2019. doi:10.1016/j.neuron.2019.02.029
  11. Ren W, Centeno MV, Berger S, et al. The indirect pathway of the nucleus accumbens shell amplifies neuropathic pain. *Nat Neurosci*. 2016;19(2):220-222. doi:10.1038/nn.4199
  12. Lobo MK, Covington 3rd HE, Chaudhury D, et al. Cell type-specific loss of BDNF

- signaling mimics optogenetic control of cocaine reward. *Science* (80- ).  
2010;330(6002):385-390. doi:10.1126/science.1188472
13. Lobo MK, Zaman S, Damez-Werno DM, et al. DeltaFosB induction in striatal medium spiny neuron subtypes in response to chronic pharmacological, emotional, and optogenetic stimuli. *J Neurosci*. 2013;33(47):18381-18395. doi:10.1523/JNEUROSCI.1875-13.2013
  14. Chandra R, Francis TC, Konkalmatt P, et al. Opposing Role for Egr3 in Nucleus Accumbens Cell Subtypes in Cocaine Action. *J Neurosci*. 2015;35(20):7927-7937. doi:10.1523/JNEUROSCI.0548-15.2015
  15. Bertran-Gonzalez J, Bosch C, Maroteaux M, et al. Opposing patterns of signaling activation in dopamine D1 and D2 receptor-expressing striatal neurons in response to cocaine and haloperidol. *J Neurosci*. 2008;28(22):5671-5685. doi:10.1523/jneurosci.1039-08.2008
  16. Bock R, Shin JH, Kaplan AR, et al. Strengthening the accumbal indirect pathway promotes resilience to compulsive cocaine use. *Nat Neurosci*. 2013;16(5):632-638. doi:10.1038/nn.3369
  17. Lobo MK, Nestler EJ. The striatal balancing act in drug addiction: distinct roles of direct and indirect pathway medium spiny neurons. *Front Neuroanat*. 2011;5:41. doi:10.3389/fnana.2011.00041
  18. Grueter BA, Robison AJ, Neve RL, Nestler EJ, Malenka RC. FosB differentially modulates nucleus accumbens direct and indirect pathway function. *Proc Natl Acad Sci U S A*. 2013;110(5):1923-1928. doi:10.1073/pnas.1221742110
  19. MacAskill AF, Cassel JM, Carter AG. Cocaine exposure reorganizes cell type- and input-specific connectivity in the nucleus accumbens. *Nat Neurosci*. 2014;17(9):1198-1207.

doi:10.1038/nm.3783

20. Kim J, Park BH, Lee JH, Park SK, Kim JH. Cell type-specific alterations in the nucleus accumbens by repeated exposures to cocaine. *Biol Psychiatry*. 2011;69(11):1026-1034. doi:10.1016/j.biopsych.2011.01.013
21. Finck BN, Kelly DP. PGC-1 coactivators: inducible regulators of energy metabolism in health and disease. *J Clin Invest*. 2006;116(3):615-622. doi:10.1172/JCI27794
22. Lin J, Handschin C, Spiegelman BM. Metabolic control through the PGC-1 family of transcription coactivators. *Cell Metab*. 2005;1(6):361-370. doi:10.1016/j.cmet.2005.05.004
23. Divakaruni SS, Van Dyke AM, Chandra R, et al. Long-Term Potentiation Requires a Rapid Burst of Dendritic Mitochondrial Fission during Induction. *Neuron*. 2018:1-16. doi:10.1016/j.neuron.2018.09.025
24. Li Z, Okamoto KI, Hayashi Y, Sheng M. The importance of dendritic mitochondria in the morphogenesis and plasticity of spines and synapses. *Cell*. 2004;119(6):873-887. doi:10.1016/j.cell.2004.11.003
25. Bobadilla A-C, Heinsbroek JA, Gipson CD, et al. Corticostriatal plasticity, neuronal ensembles, and regulation of drug-seeking behavior. *Prog Brain Res*. 2017;235:93-112. doi:10.1016/bs.pbr.2017.07.013
26. Cahill ME, Walker DM, Gancarz AM, et al. The dendritic spine morphogenic effects of repeated cocaine use occur through the regulation of serum response factor signaling. *Mol Psychiatry*. 2017;23:1474. <https://doi.org/10.1038/mp.2017.116>.
27. Wolf ME. Synaptic mechanisms underlying persistent cocaine craving. *Nat Rev Neurosci*. 2016;17(6):351-365. doi:10.1038/nrn.2016.39

28. Ferrario CR, Gorny G, Crombag HS, Li Y, Kolb B, Robinson TE. Neural and behavioral plasticity associated with the transition from controlled to escalated cocaine use. *Biol Psychiatry*. 2005;58(9):751-759. doi:10.1016/j.biopsych.2005.04.046
29. Gipson CD, Kupchik YM, Kalivas PW. Rapid, transient synaptic plasticity in addiction. *Neuropharmacology*. 2014;76(PART B):276-286. doi:10.1016/j.neuropharm.2013.04.032
30. Norrholm SD, Bibb JA, Nestler EJ, Ouimet CC, Taylor JR, Greengard P. Cocaine-induced proliferation of dendritic spines in nucleus accumbens is dependent on the activity of cyclin-dependent kinase-5. *Neuroscience*. 2003;116(1):19-22.
31. Robinson TE, Kolb B. Structural plasticity associated with exposure to drugs of abuse. *Neuropharmacology*. 2004;47 Suppl 1:33-46. doi:10.1016/j.neuropharm.2004.06.025
32. Wang X, Cahill ME, Werner CT, et al. Kalirin-7 mediates cocaine-induced AMPA receptor and spine plasticity, enabling incentive sensitization. *J Neurosci*. 2013;33(27):11012-11022. doi:10.1523/JNEUROSCI.1097-13.2013
33. Gancarz AM, Wang ZJ, Schroeder GL, et al. Activin receptor signaling regulates cocaine-primed behavioral and morphological plasticity. *Nat Neurosci*. 2015;18(7):959-961. doi:10.1038/nn.4036
34. Engeln M, Mitra S, Chandra R, et al. Sex-Specific Role for Egr3 in Nucleus Accumbens D2-Medium Spiny Neurons Following Long-Term Abstinence From Cocaine Self-administration. *Biol Psychiatry*. 2020;87(11):992-1000. doi:10.1016/j.biopsych.2019.10.019
35. Gerfen CR, Paletzki R, Heintz N. GENSAT BAC cre-recombinase driver lines to study the functional organization of cerebral cortical and basal ganglia circuits. *Neuron*. 2013. doi:10.1016/j.neuron.2013.10.016

36. Chandra R, Calarco CA, Lobo MK. Differential mitochondrial morphology in ventral striatal projection neuron subtypes. *J Neurosci Res.* 2019;97(12):1579-1589.  
doi:10.1002/jnr.24511
37. Golden SA, Christoffel DJ, Heshmati M, et al. Epigenetic regulation of RAC1 induces synaptic remodeling in stress disorders and depression. *Nat Med.* 2013;19(3):337-344.  
doi:10.1038/nm.3090
38. Robison AJ, Vialou V, Mazei-Robison M, et al. Behavioral and structural responses to chronic cocaine require a feedforward loop involving  $\Delta$ FosB and calcium/calmodulin-dependent protein kinase II in the nucleus accumbens shell. *J Neurosci.* 2013;33(10):4295-4307. doi:10.1523/JNEUROSCI.5192-12.2013
39. Maze I, Covington HE 3rd, Dietz DM, et al. Essential role of the histone methyltransferase G9a in cocaine-induced plasticity. *Science.* 2010;327(5962):213-216.  
doi:10.1126/science.1179438
40. Russo SJ, Dietz DM, Dumitriu D, Morrison JH, Malenka RC, Nestler EJ. The addicted synapse: mechanisms of synaptic and structural plasticity in nucleus accumbens. *Trends Neurosci.* 2010;33(6):267-276. doi:10.1016/j.tins.2010.02.002
41. Feng J, Wilkinson M, Liu X, et al. Chronic cocaine-regulated epigenomic changes in mouse nucleus accumbens. *Genome Biol.* 2014;15(4):R65. doi:10.1186/gb-2014-15-4-r65
42. Hoppins S. The regulation of mitochondrial dynamics. *Curr Opin Cell Biol.* 2014.  
doi:10.1016/j.ceb.2014.03.005
43. Falkenberg M, Gaspari M, Rantanen A, Trifunovic A, Larsson NG, Gustafsson CM. Mitochondrial transcription factors B1 and B2 activate transcription of human mtDNA. *Nat Genet.* 2002. doi:10.1038/ng909



44. Hällberg BM, Larsson NG. Making proteins in the powerhouse. *Cell Metab.* 2014.  
doi:10.1016/j.cmet.2014.07.001
45. Friedman JR, Nunnari J. Mitochondrial form and function. *Nature.* 2014;505(7483):335-343. doi:10.1038/nature12985
46. Baker MJ, Frazier AE, Gulbis JM, Ryan MT. Mitochondrial protein-import machinery: correlating structure with function. *Trends Cell Biol.* 2007. doi:10.1016/j.tcb.2007.07.010
47. Chen YH, Huang EYK, Kuo TT, Miller J, Chiang YH, Hoffer BJ. Impact of traumatic brain injury on dopaminergic transmission. *Cell Transplant.* 2017.  
doi:10.1177/0963689717714105
48. Francis TC, Chandra R, Gaynor A, et al. Molecular basis of dendritic atrophy and activity in stress susceptibility. *Mol Psychiatry.* 2017;22:1512.  
<https://doi.org/10.1038/mp.2017.178>.
49. Galvan L, André VM, Wang EA, Cepeda C, Levine MS. Functional Differences Between Direct and Indirect Striatal Output Pathways in Huntington's Disease. *J Huntingtons Dis.* 2012;1:17-25. doi:10.3233/JHD-2012-120009
50. Pascoli V, Terrier J, Espallergues J, Valjent E, O'Connor EC, Luscher C. Contrasting forms of cocaine-evoked plasticity control components of relapse. *Nature.* 2014;509(7501):459-464. doi:10.1038/nature13257

## Figure Legends

**Figure 1. Cocaine-induced Egr3 binding to promoters of mitochondrial-related nuclear gene in NAc.** (A) Illustration of the ChIP assay using anti-Egr3 to immunoprecipitate chromatin in NAc tissue. (B) **Top panel:** The timeline of cocaine (20mg/kg, i.p.) or saline injections and NAc tissue collection after 24-hour abstinence. **Bottom panel:** Egr3 binding is increased on Drp1, Nrf2 and Poly gene promoters in NAc in the cocaine group compared to saline injected mice. Student's t test, \* $p < 0.05$ ;  $n = 3-7$  in per group. Error bars, SEM.

**Figure 2. Cocaine induced mitochondrial-related nuclear gene expression in NAc of rodents and human subjects.** (A) Mice treated with 7 days of cocaine (20mg/kg, ip) display higher mRNA expression of nrf1, nrf2 and tomm20 genes 24h in NAc. Student's t-test, \* $p < 0.05$ , \*\*\* $p < 0.001$ ;  $n = 5-6$  saline and  $n = 6-7$  cocaine group. (B) Rat mRNA expression in NAc tissue after 10 days self-administration (**upper panel**) followed by 24hr abstinence. **Bottom panel:** increased expression of nrf1, tfb1 and tomm20 in NAc of rats that self-administer cocaine compared to saline. Student's t test, \* $p < 0.05$ ;  $n = 5$  saline and  $n = 6$  cocaine. (C) mRNA expression in human postmortem NAc tissue indicated that Nrf2 gene expression is higher in human cocaine dependents compared to control subjects. Student's t test, \* $p < 0.05$ ;  $n = 14-16$  control and  $n = 13-15$  cocaine dependent. Error bars, SEM.

**Figure 3. Ribosome associated mitochondrial-related mRNA are altered in NAc MSN**

**subtypes after repeated cocaine.**(A) Illustration of NAc D1-MSN (blue) and D2-MSN (red)

subtypes and the RiboTag procedure to isolate ribosome-associated mRNA from MSN subtypes using D1-Cre-RT and D2-Cre-RT mice. HA tagged (green) ribosomes are immunoprecipitated from NAc homogenates using anti-HA coupled to magnetic beads, followed by isolation of ribosome-associated mRNA from D1-MSNs and D2-MSNs). **(B) Top panel:** The timeline of cocaine (20mg/kg, i.p.) or saline injections and NAc tissue collection after 24-hour abstinence.

**Bottom panel:** tfam ribosome-associated mRNA is increased in D1-MSNs Student's t-test,

\* $p < 0.05$ ;  $p = 0.07$  nrf2;  $p = 0.052$  tomm20;  $n = 4-6$  each group. **(C)** Poly $\gamma$ , tfam, tfb1 and tomm20

expression is reduced in D2-MSNs after repeated cocaine (7 days, 20mg/kg). Student's t-test,

\* $p < 0.05$ ; \*\* $p < 0.01$ ; \*\*\* $p < 0.001$ ;  $n = 5$  in saline and  $n = 5-6$  in cocaine group, Error bars, SEM.

**Figure 4. Mitochondrial-related nuclear gene expression in NAc after Egr3 overexpression**

**in MSN subtypes.** (A) Top-The timeline of cocaine (20mg/kg, i.p.) or saline injections and NAc

tissue collection after 24-hour abstinence. Bottom- Differential expression of mitochondrial-related nuclear genes illustrating that Drp1, PGC1 $\alpha$ , tfam and tomm20 mRNA was increased after Egr3 overexpression in D1-MSNs and cocaine exposure compared to EYFP controls.

Student's t-test, \* $p < 0.05$ ;  $n = 4-5$  in each group. **(B)** Mitochondrial-related nuclear genes are

unaltered in NAc after Egr3 overexpression in D2-MSNs. Student's t-test,  $n = 3-6$  in control and 4-9 Egr3 OE group, Error bars, SEM.

**Figure 5. Cocaine induced Drp1 and PGC1 $\alpha$  gene expression is blocked by Egr3 reduction**

**in D1-MSNs.** (A) The timeline of Egr3-miR virus surgery followed by cocaine (20mg/kg, i.p.) or

saline injections and NAc tissue collection after 24-hour abstinence. **(B)** Drp1 and PGC1 $\alpha$  mRNAs are reduced in D1-MSN of the Egr3miR cocaine group compared to the SS-miR cocaine group. Two way ANOVA: Drp1; Interaction  $F_{(1,20)} = 12.67$ ; Post hoc test  $p = 0.002$ , \*\* $p < 0.01$ ; \*\*\* $p < 0.001$ ;  $n = 5$  SS-miR Saline,  $n = 6$  SS-miR Cocaine,  $n = 6$  Egr3-miR Saline,  $n = 7$  Egr3-miR cocaine. Two-way ANOVA: PGC1 $\alpha$  ; Interaction  $F_{(1,18)} = 9.398$ ; Post hoc test  $p = 0.0067$ , \* $p < 0.05$ ;  $n = 5$  SS-miR Saline,  $n = 5$  SS-miR Cocaine,  $n = 6$  Egr3-miR Saline,  $n = 6$  Egr3-miR cocaine. Error bars, SEM.

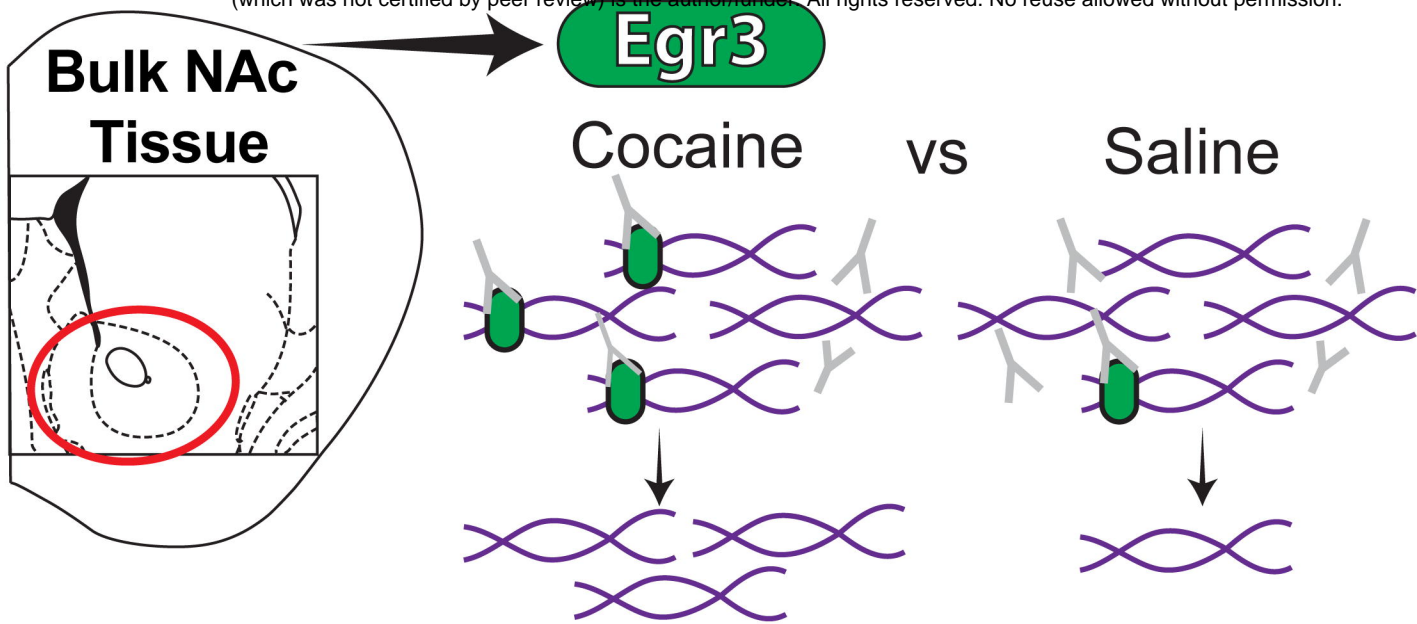
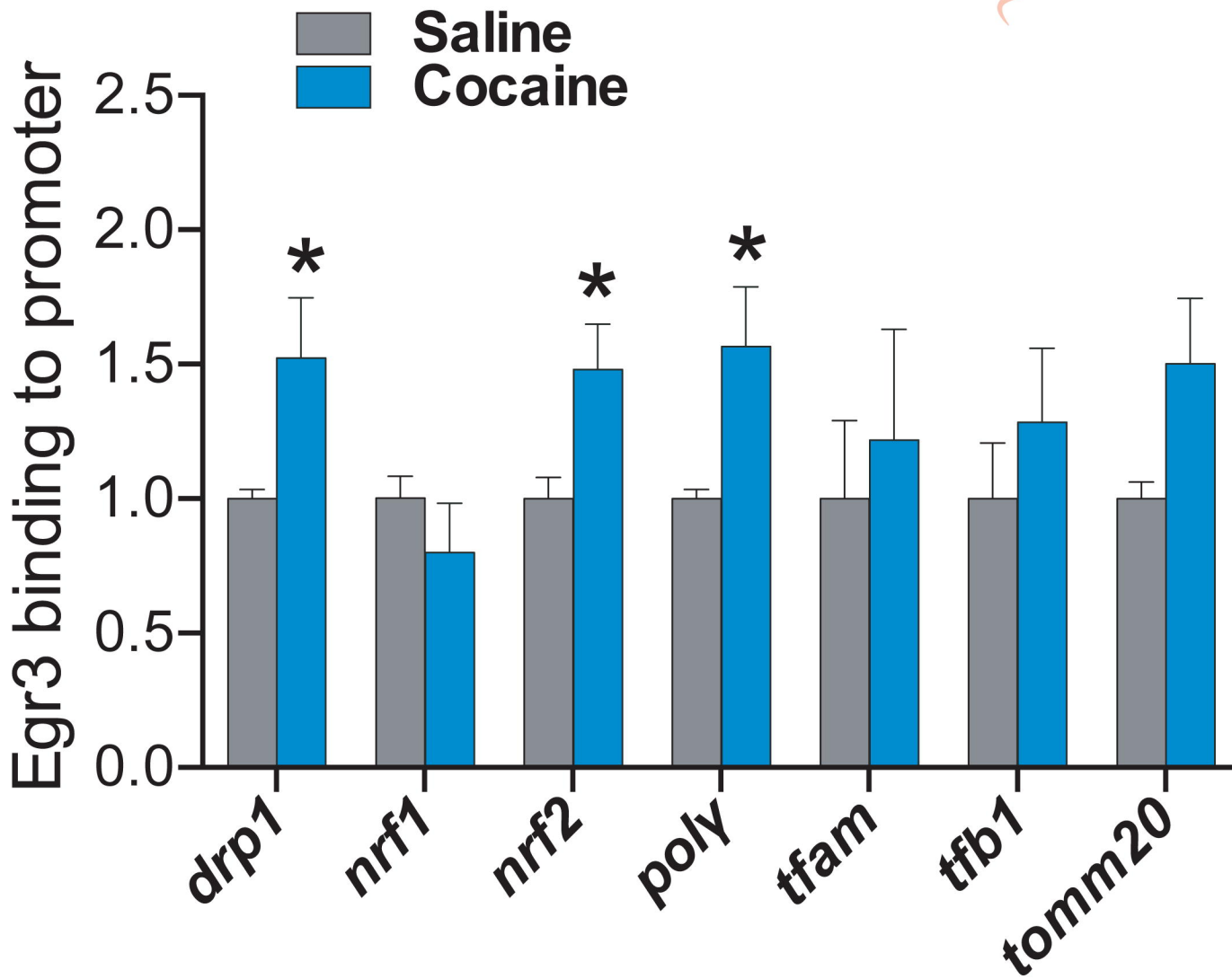
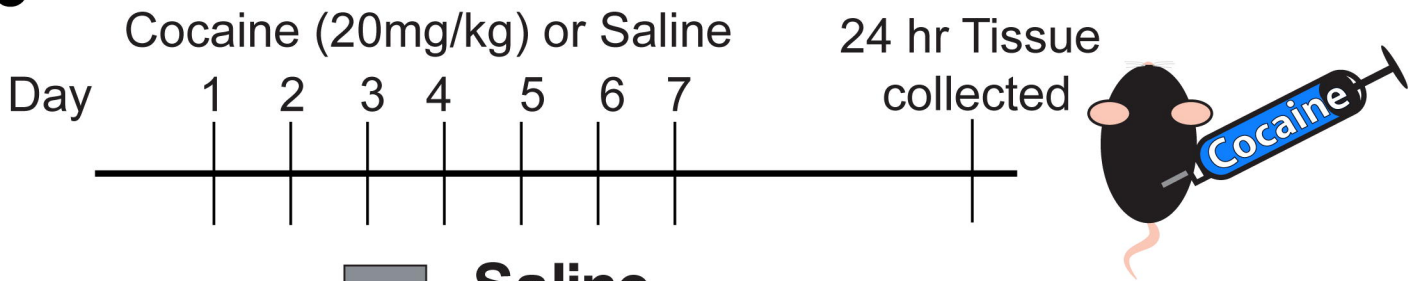
**Figure 6. Egr3 knockdown attenuates cocaine-mediated induction of small sized mitochondria in D1-MSN dendrites.** **(A)** The timeline of Egr3-miR virus surgery followed by cocaine (20mg/kg, i.p.) or saline injections and NAc tissue collection after 24-hour abstinence. **(B)** Representative images for D1-MSN dendrites (green) with labeled mitochondria (red) after repeated cocaine exposure from SS-miR and Egr3-miR groups. **(C)** 3D reconstruction of dendrites and mitochondria highlights an increase in the frequency of smaller length mitochondria in D1-MSN dendrites in the cocaine SS-miR group, which is attenuated in the Egr3- miR cocaine group. The Egr3-miR cocaine group displayed a decrease in the frequency of smaller size mitochondria in the 1.5-3 $\mu$ m size bracket compared to the SS-miR cocaine group. Two-way ANOVA: Interaction:  $F_{(15,70)} = 5.069$ ,  $P < 0.0001$ , Bonferroni post hoc: \* $p < 0.05$ , \*\* $p < 0.01$ , \*\*\* $p < 0.001$ ;  $n = 4-5$ . **(D)** Mitochondrial density (per dendrite 10 mm length) is unaltered in D1-MSNs of mice exposed to cocaine and Egr3-miR. Two-way ANOVA:  $F_{(1,14)} = 0.1603$ ;  $p = 0.6949$ ;  $n = 4-5$  each group. **(E)** Mitochondrial index (mitochondrial length per 10 $\mu$ m of dendrite length) in Egr3 knockdown compared to control group demonstrating no change among the four groups. Two-way ANOVA  $F_{(1,14)} = 0.04760$ ;  $p = 0.8304$ .  $n = 4-5$  per group **(F)**

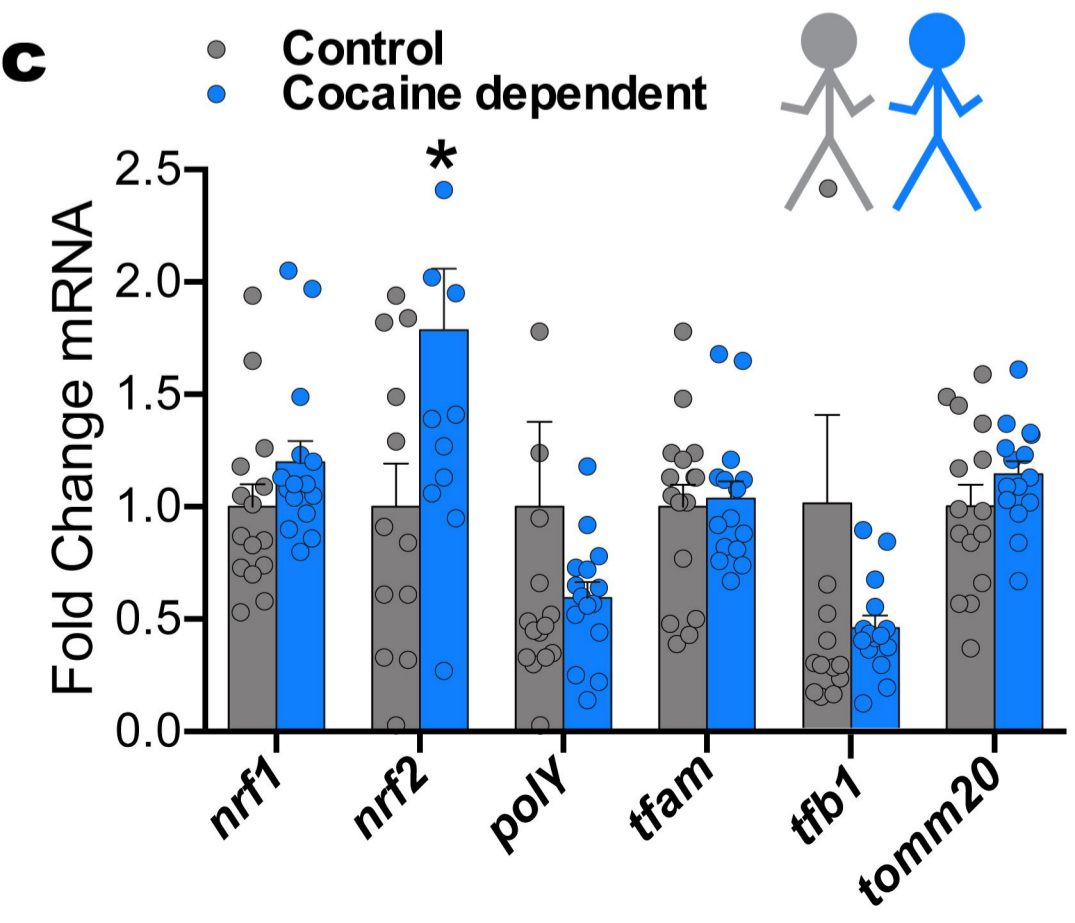
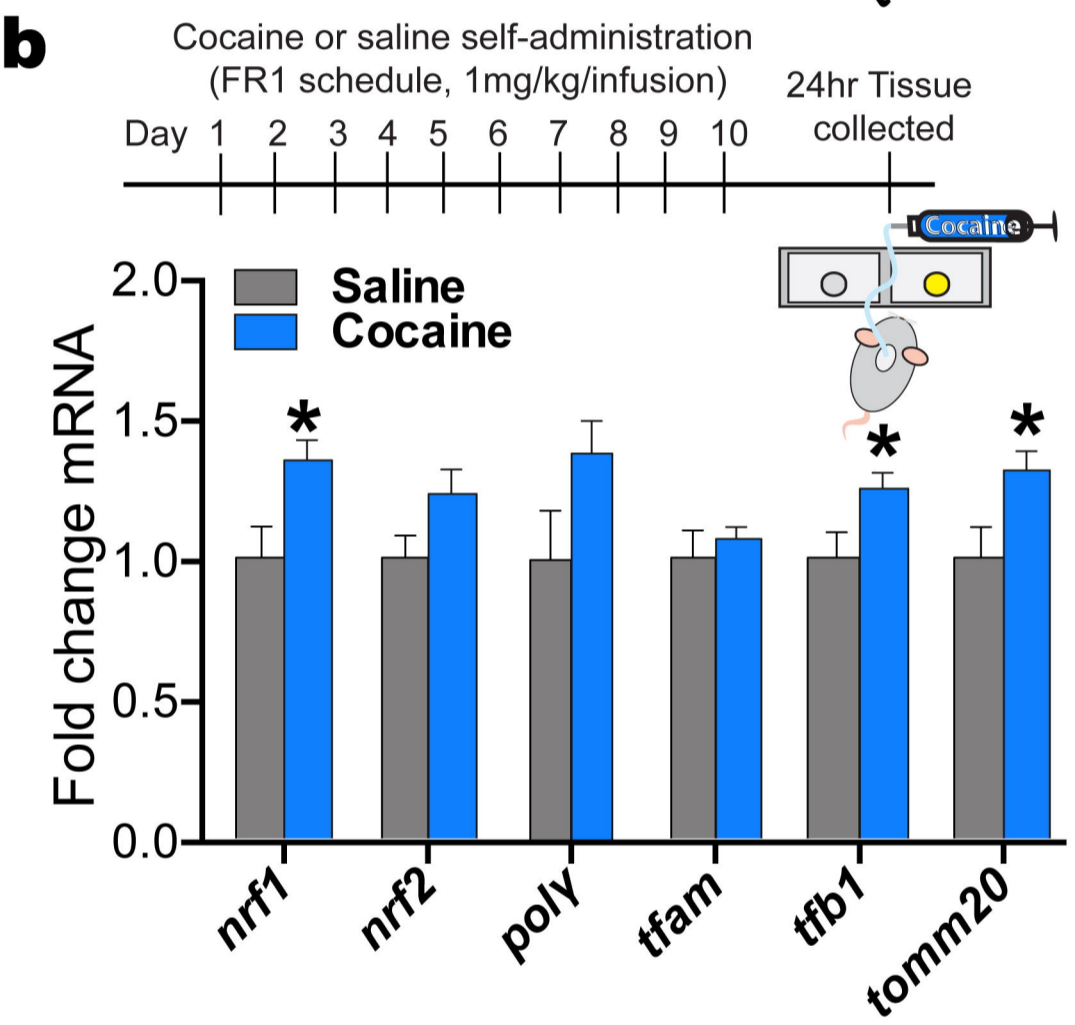
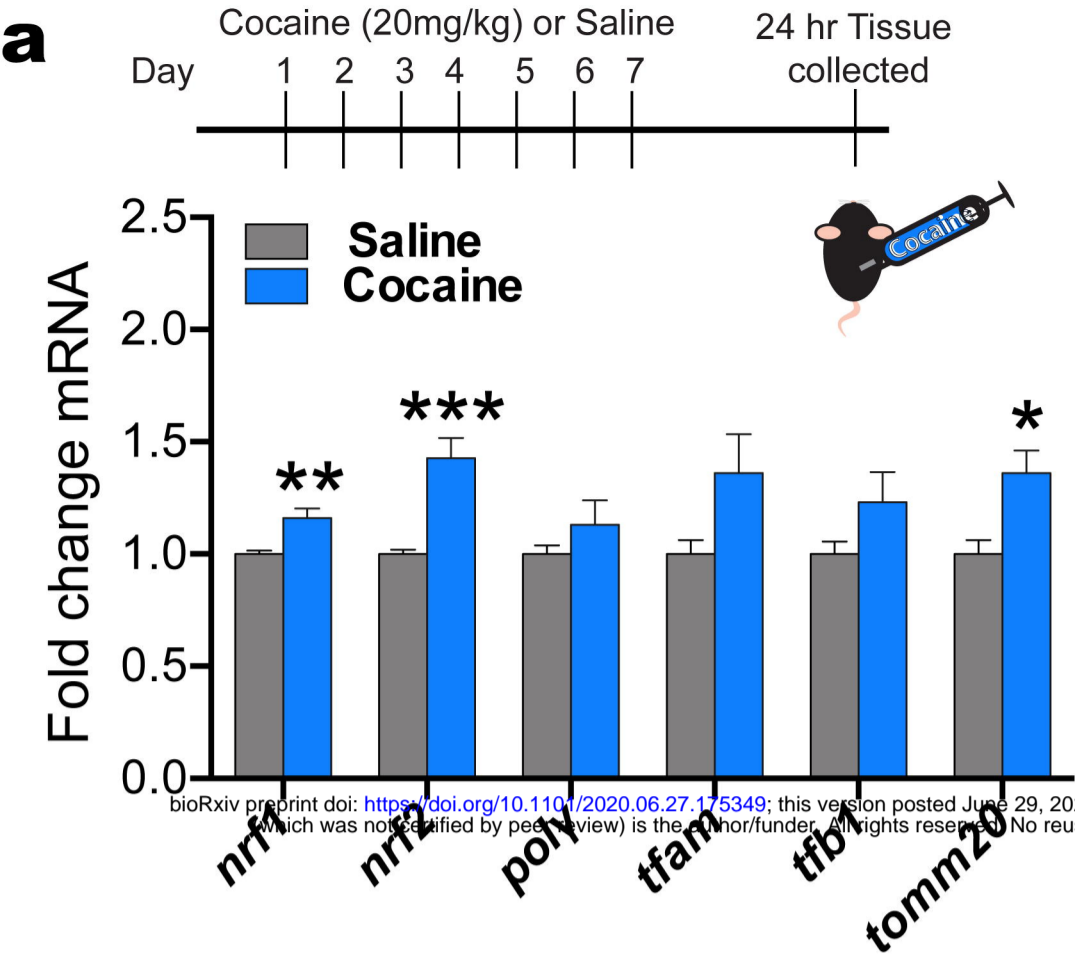
Mitochondrial volume ratio (Relative to dendrite volume) is enhanced in the SS-miR cocaine group compared to the Egr3-miR saline group. Two-way ANOVA  $F_{(1,14)}=0.4792$ ;  $p= 0.5001$ ;  $n=4-5$  per group. Error bars, SEM.

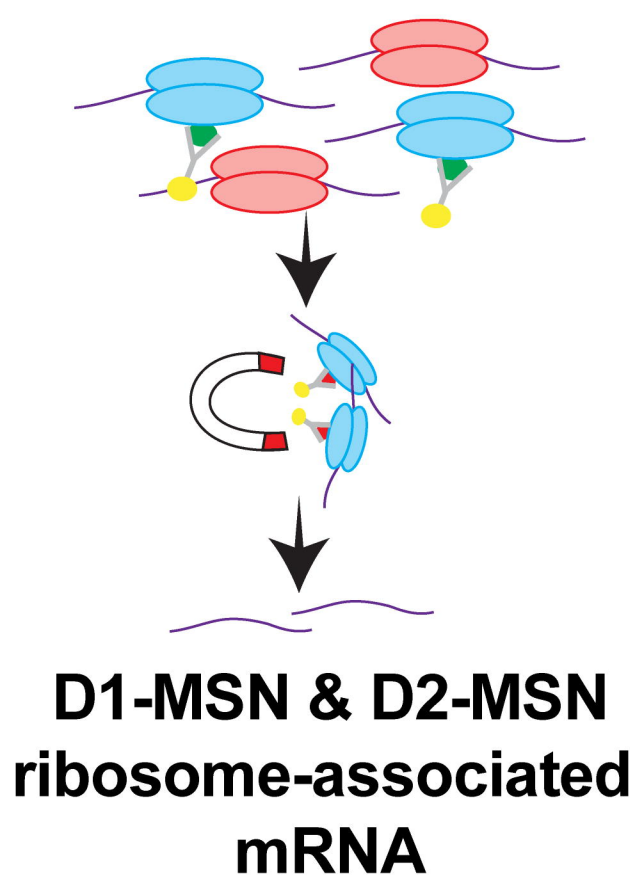
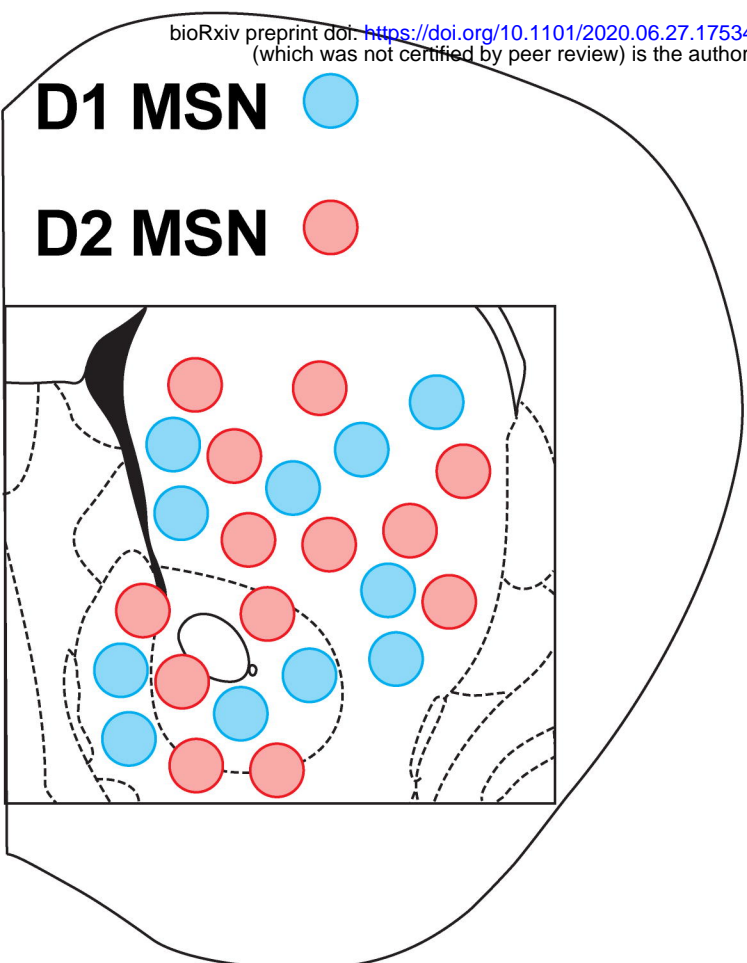
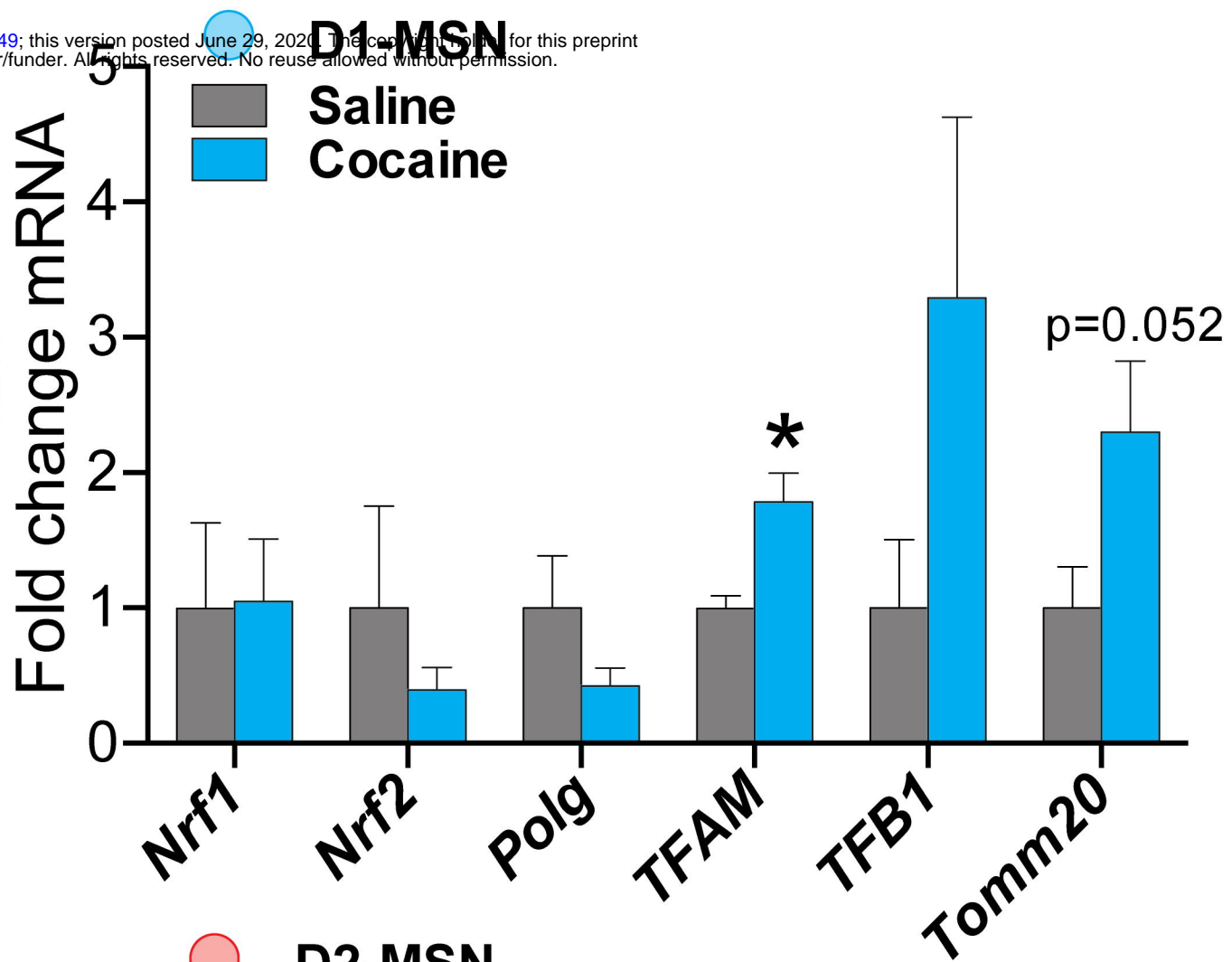
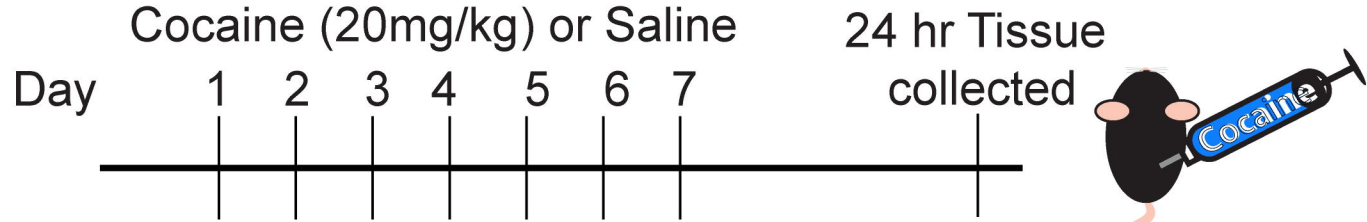
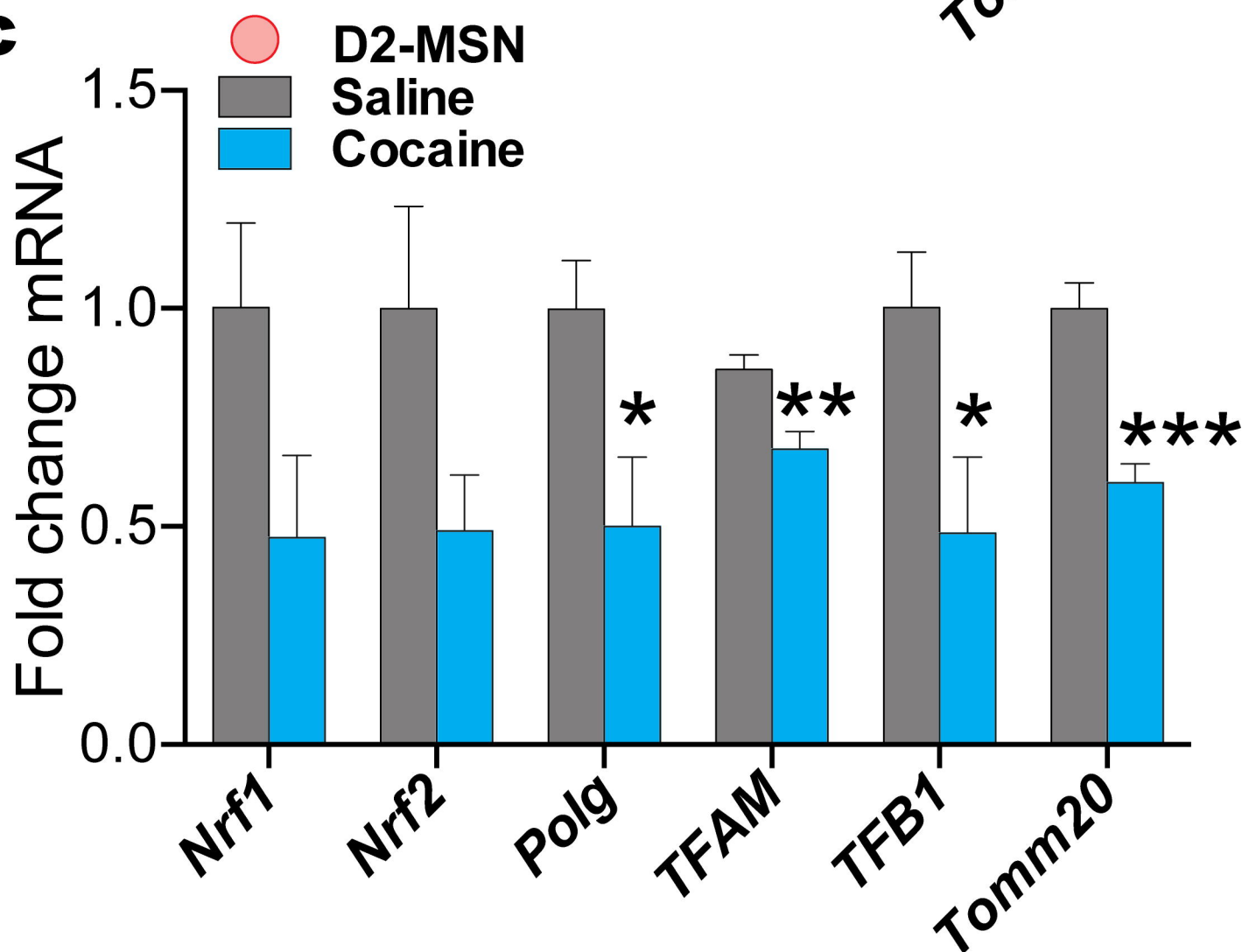
**Table 1. Mitochondrial gene regulation by species, administration, and neuron subpopulation.**

**a**

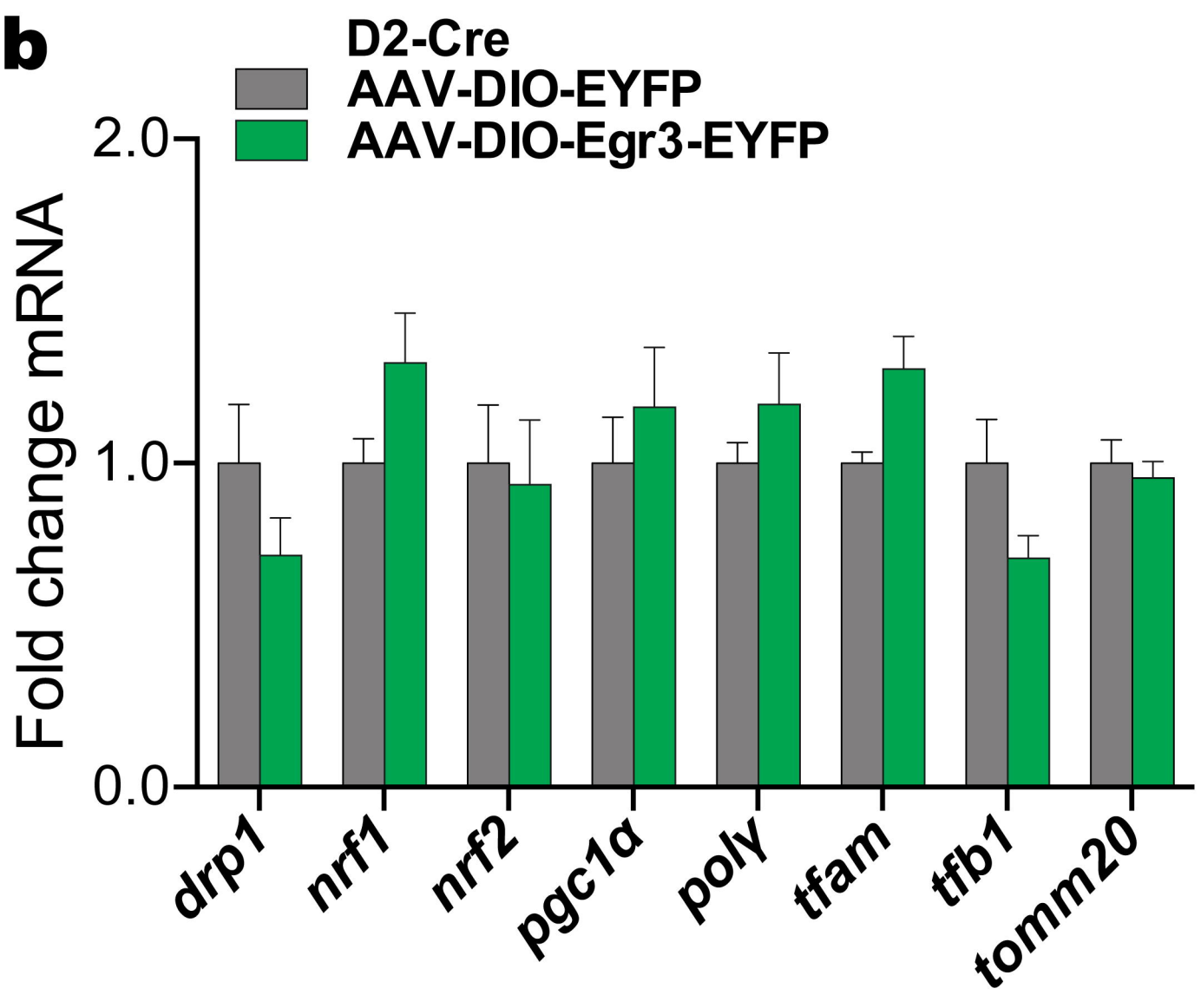
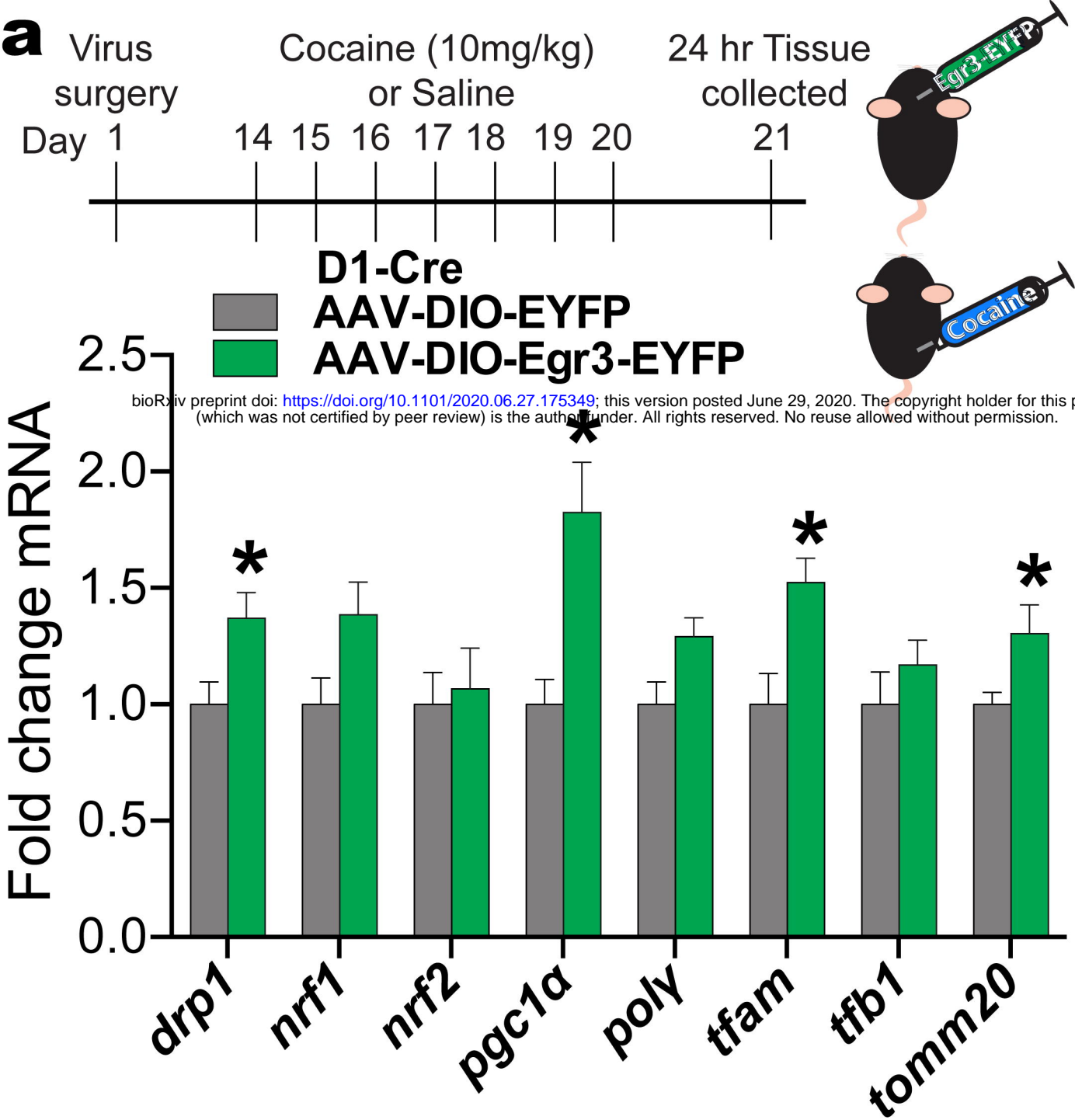
bioRxiv preprint doi: <https://doi.org/10.1101/2020.06.27.175349>; this version posted June 29, 2020. The copyright holder for this preprint (which was not certified by peer review) is the author/funder. All rights reserved. No reuse allowed without permission.

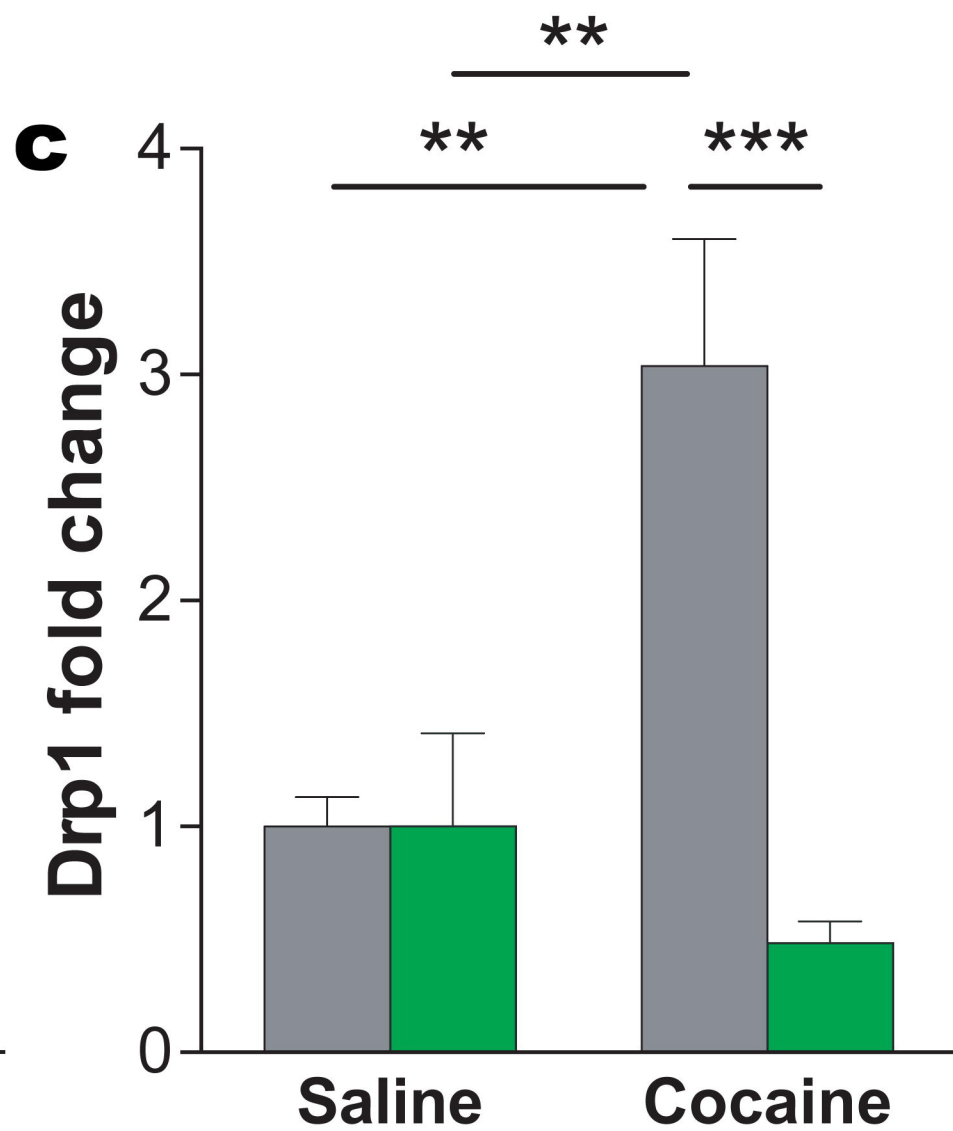
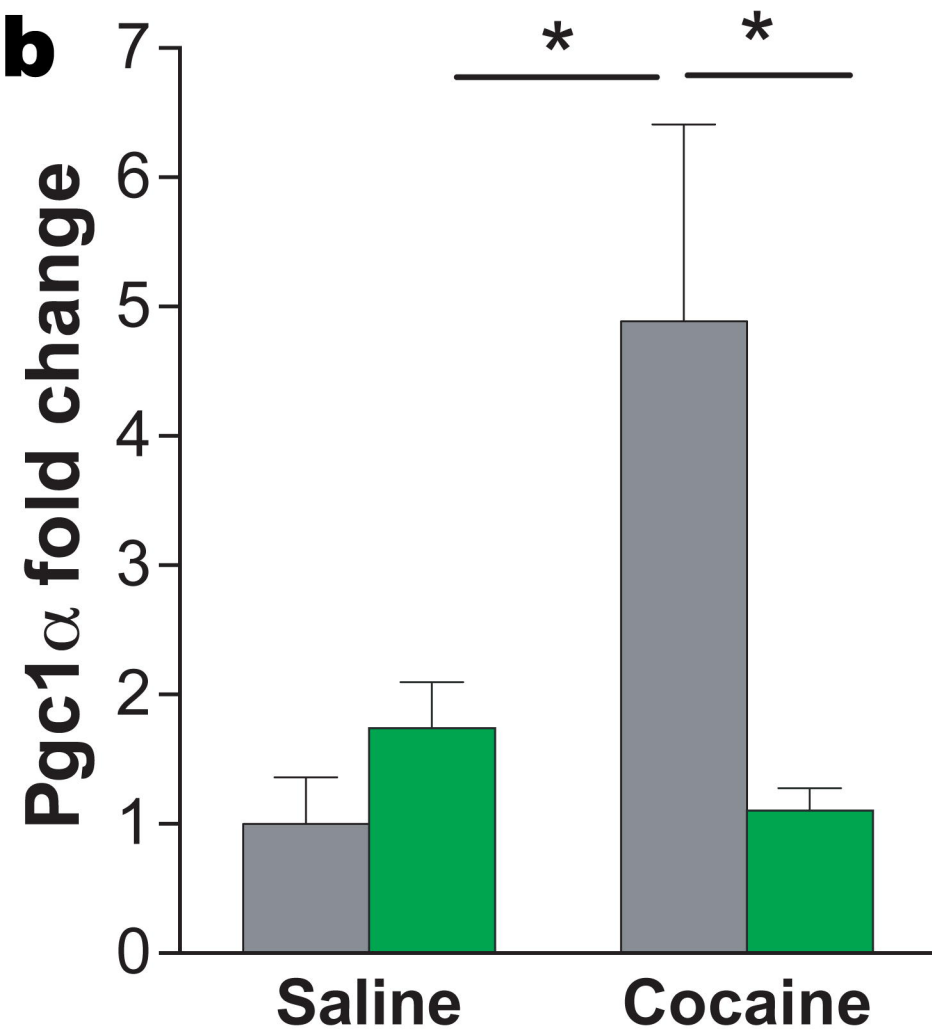
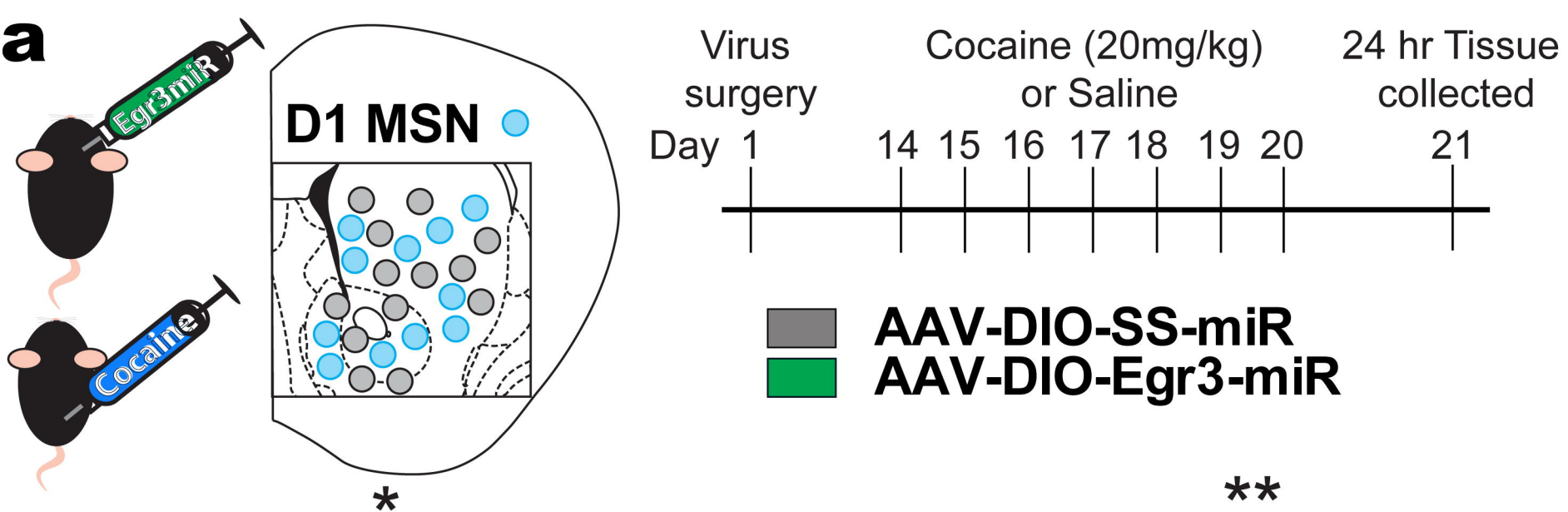
**b**

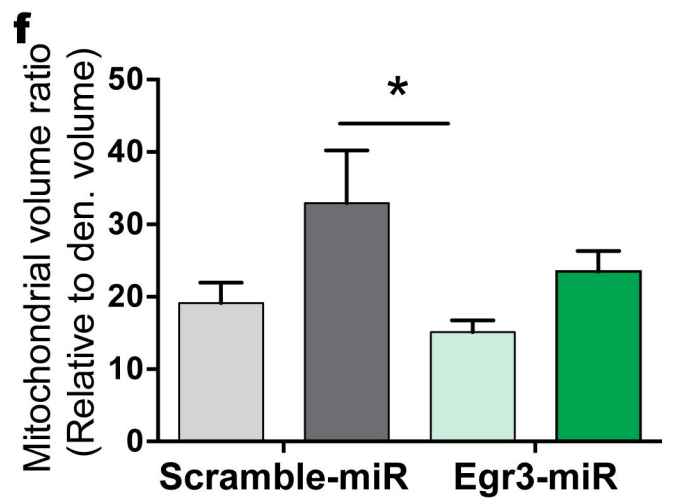
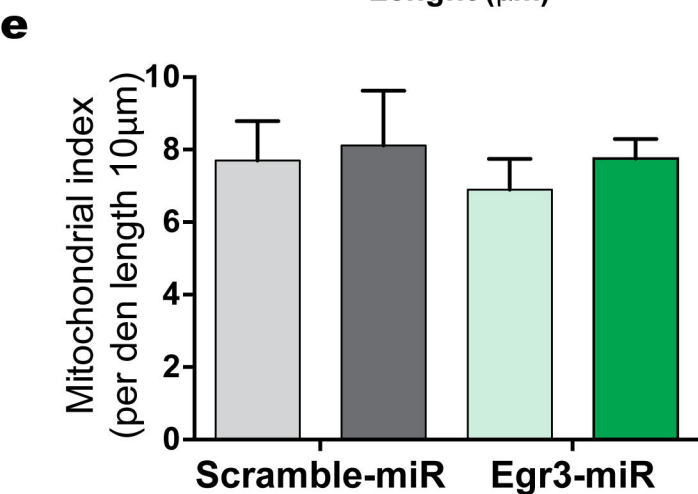
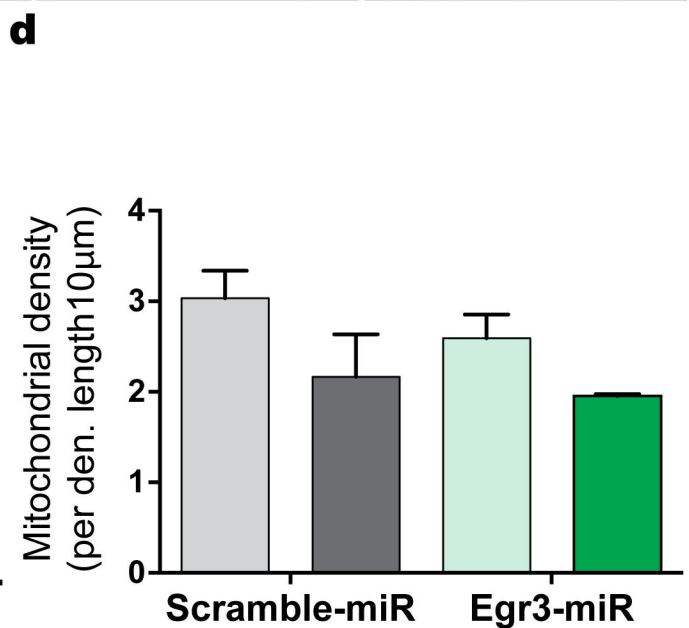
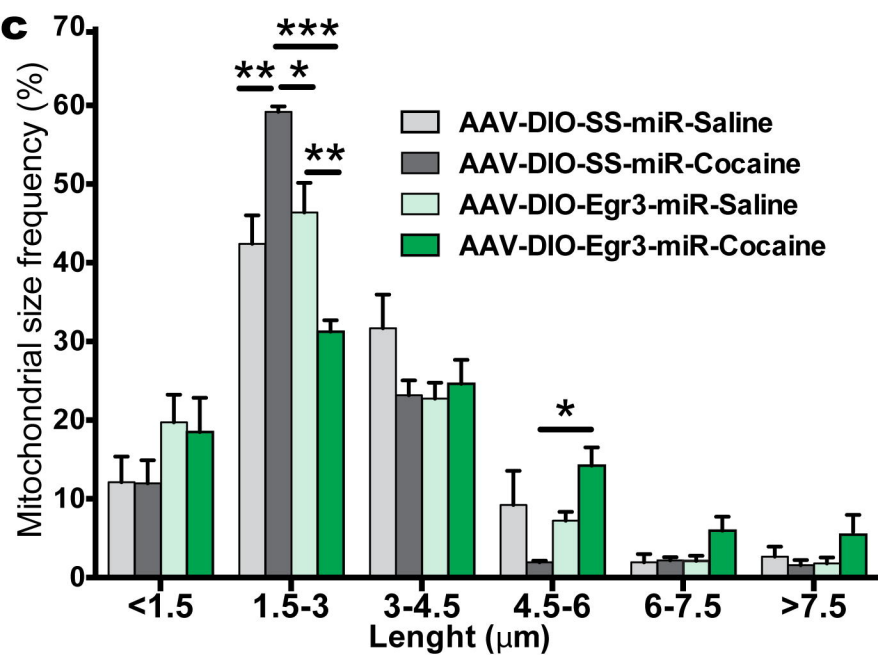
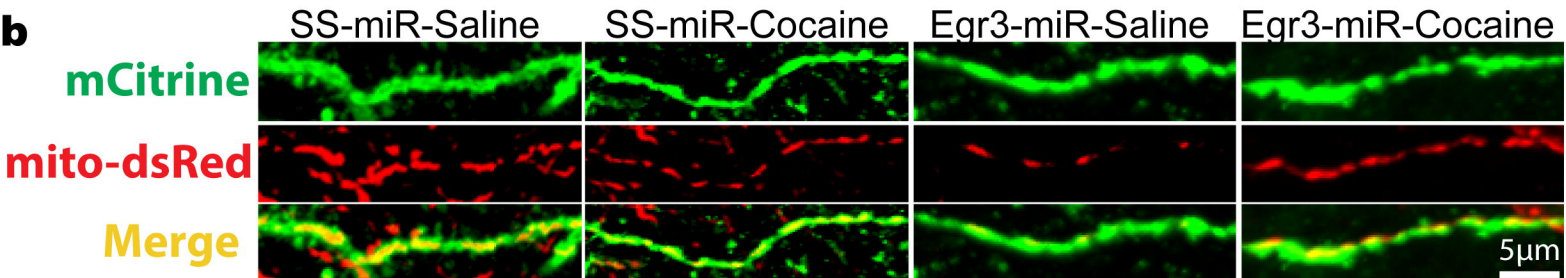
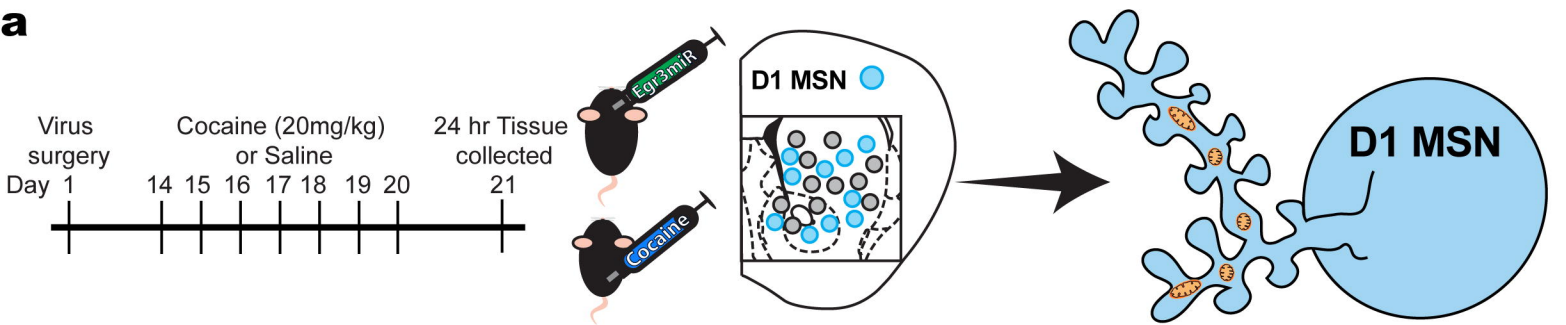


**a****b****c**









	Species	nrf1	nrf2	tfam	tfb1	poly	tomm20	Egr3	PGC1 $\alpha$	Drp1
<b>Total Brain</b>	human	-	↑	-	↑	↓	↓	N/A	N/A	↑ <sup>3</sup>
	rat (i.p.)	↑	-	-	↑	-	-	↓ <sup>1</sup>	N/A	↑ <sup>3</sup>
	mouse (i.p.)	↑	↑	-	↑	-	-	↓ <sup>1</sup>	↑ <sup>2</sup>	↑ <sup>3</sup>
<b>D1 MSN</b>	mouse (i.p.)	-	-	↑	-	-	-	↑ <sup>1</sup>	↑ <sup>2</sup>	↑ <sup>3</sup>
<b>D2 MSN</b>	mouse (i.p.)	-	-	↑	↓	↓	↓	↓ <sup>1</sup>	↓ <sup>2</sup>	↓ <sup>3</sup>

<sup>1</sup>Chandra, R., et al., (2015). *Journal of Neuroscience*, 35(20), 7927–7937

<sup>2</sup>Chandra, R., et al., (2017). *Neuron*, 96(6), 1327-1341.e6

<sup>3</sup>Chandra, R., et al., (2017). *Biological Psychiatry*, 81(7), 564-572